

A STUDY OF THE LIQUID-VAPOR PHASE CHANGE OF
MERCURY BASED ON IRREVERSIBLE THERMODYNAMICS

by

Robert Roy Adt, Jr.

S.B., University of Miami
(1962)

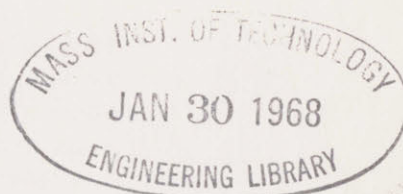
S.M., Massachusetts Institute of Technology
(1965)

Submitted in Partial Fulfillment
of the Requirements for the
Degree of Doctor of
Science

at

Massachusetts Institute of
Technology

June 1967

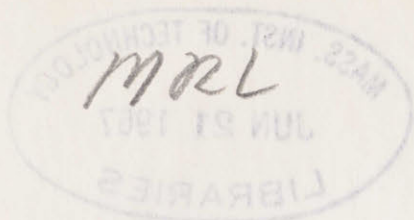


Signature redacted

Signature of Author
Department of Mechanical Engineering, June 1, 1967

Certified by
Thesis Supervisor

Accepted by
Chairman, Departmental Committee
on Graduate Students



A STUDY OF THE LIGHT-VAPOUR PRESS CHANGE OF
MERCURY BASED ON IRRADIATION EXPERIMENTATION

by

Robert H. Ash, Jr.

Thesis

M. E.

S. B. U. of Mass.

1967
Sci.

S. M., Massachusetts Institute of Technology
(1967)

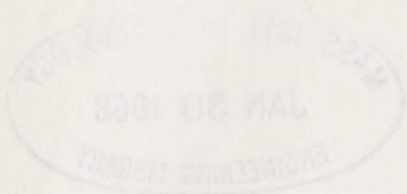
Submitted in Partial Fulfillment
of the Requirements for the
Degree of Doctor of
Science

at

Massachusetts Institute of

Technology

June 1967



Signature of Author
Department of Mechanical Engineering, June 1, 1967

Certified by
Thesis Supervisor

Accepted by
Chairman, Departmental Committee
on Graduate Students

A STUDY OF THE LIQUID-VAPOR PHASE CHANGE OF
MERCURY BASED ON IRREVERSIBLE THERMODYNAMICS

by

Robert Roy Adt, Jr.

Submitted to the Department of Mechanical Engineering on June 1, 1967,
in partial fulfillment of the requirement for the degree of Doctor of
Science.

ABSTRACT

The object of this work is to experimentally and theoretically investigate the transport coefficients which appear in the previously obtained linear irreversible-thermodynamic rate equations of a phase change. An experiment which involves the steady-state evaporation of mercury was performed to measure the principal transport coefficient appearing in the mass-rate equation and the coupling transport coefficient appearing in both the mass-rate equation and the energy-rate equation.

The principal transport coefficient ∇ , usually termed the "condensation" or "evaporation" coefficient is found to be approximately 0.9 which is higher than that measured previously in condensation experiments.

The experimental value of the coupling coefficient K does not agree with the value predicted from Schrage's kinetic analysis of the phase change. A modified kinetic analysis in which the Onsager reciprocal law and the conservation laws are invoked is presented which removes this discrepancy and which shows that the use of Schrage's equation for predicting mass rates of phase change is a good approximation.

Thesis Supervisor: Doctor George N. Hatsopoulos
Title: Senior Lecturer in Mechanical Engineering

ACKNOWLEDGMENTS

I sincerely thank:

Dr. George N. Hatsopoulos, my thesis supervisor, for his encouragement and expert advice.

Professors Walter J. Bornhorst, S. William Gouse, Jr., Peter Griffith, and Warren M. Rohsenow, members of my thesis committee, for their time and effort.

Dr. Detlev G. Kroger and Professor Edwin J. Le Fevre for many valuable discussions.

Barbara, my wife, for her patience and encouragement during the course of this work.

Miss Lucille Blake for typing this thesis.

Mr. Ravinder Sakhuja for assistance in some of the experimental work.

This work is an outgrowth of Professor Bornhorst's Doctoral Thesis, and I should like to extend a special word of thanks to him for many invaluable discussions, many contributions, and constant encouragement.

This work was supported by the National Aeronautics and Space Administration under contract number NAS8-20013 and was done in part at the Computation Center at the Massachusetts Institute of Technology, Cambridge, Massachusetts.

TABLE OF CONTENTS

	Page
ABSTRACT	2
ACKNOWLEDGMENTS	3
TABLE OF CONTENTS	4
LIST OF ILLUSTRATIONS	7
LIST OF SYMBOLS	8
I. INTRODUCTION	10
I-1. Nusselt's Analysis of Condensation	10
I-2. Resistance of the Liquid-Vapor Interface	10
I-3. Schrage's Kinetic Analysis of the Phase Change	11
I-4. Incorporation of Schrage's Kinetic Analysis into the Condensation Problem	13
I-5. Linear Irreversible Thermodynamic Analysis of the Phase Change	13
Meaning of the Transport Coefficient L_{ii}	14
Meaning of the Transport Coefficient L_k	15
Meaning of the Transport Coefficient K	15
I-6. Incorporation of the Thermodynamic Analysis into the Condensation Problem	18
I-7. Basic Differences Between the Thermodynamic Analysis and Schrage's Theory	18
I-8. Present Investigation	19
II. EXPERIMENTAL METHOD	20
II-1. Steady-State Evaporation Experiment	21
II-2. Equations for Steady-State Evaporation	21
III. EXPERIMENTAL APPARATUS	23
IV. EXPERIMENTAL OPERATING PROCEDURE	26
V. EXPERIMENTAL DETERMINATION OF TRANSPORT COEFFICIENTS . .	29
V-1. Relationships Between the Transport Coefficients and Measurable Quantities	29

	Page
V-2. Necessary Measurements	30
V-3. Experimental Results	32
VI. DISCUSSION OF EXPERIMENTAL RESULTS	34
VI-1. Concerning the Coefficient	34
VI-2. Concerning the Coefficient K or U	35
VII. ANALYTICAL CONSIDERATION OF THE KINETICS AND THERMODYNAMICS OF THE INTERFACE	36
VII-1. Conservation of Momentum Considerations	37
Relationship Between the Parameters Defining the Velocity Distribution	37
Momentum Considerations in Schrage's Model	40
VII-2. Use of Half Maxwellian Velocity Distributions to Completely Describe the Interface	40
Conservation of Momentum	40
Conservation of Energy	41
Kinetic Expression for J_i	42
Thermodynamic Expression for J_i	43
Discussion of the Analysis	43
VII-3. Improved Method of Modeling the Interface	44
Conservation of Momentum	45
Kinetic Expression for $(J_i)_Q, \rho=0$	45
Thermodynamic Expression for $(J_i)_Q, \rho=0$	45
Conservation of Energy	46
Calculation of L_{ii}	46
General Expression for J_i	47
Discussion of Analysis	48
Alternative Description	48
VIII. CONCLUSIONS	50
IX. RECOMMENDATIONS	51
BIBLIOGRAPHY	52

	Page
APPENDIX A - DERIVATION OF J_1 EQUATION FROM KINETIC THEORY . .	54
APPENDIX B - CONSIDERATION OF EXPERIMENTAL ERRORS	58
B-1. Uncertainty Intervals	58
B-2. Major Errors in U	58
B-3. Major Errors in σ	59
B-4. Additional Errors	60
APPENDIX C - DEVELOPMENT OF THE ALTERNATIVE DESCRIPTION (SECTION VII-3)	63
APPENDIX D - BIOGRAPHICAL NOTE	68
TABLE I - EXPERIMENTAL RESULTS	70

LIST OF ILLUSTRATIONS

Fig. No.		Page
1	Nusselt Model of Condensation	72
2	Schrage's Kinetic Model of the Phase Change	73
3	Use of Schrage's Kinetic Analysis in the Condensation Problem	74
4	No-Flow Experiment	75
5	Isothermal Experiment	76
6	Condensation Problem Including the Thermodynamic Analysis	77
7	Steady-State Evaporation Experiment	78
8	First Law Consideration of Steady-State Evaporation Experiment	79
9	Flow Diagram of Experiment	80
10	Drawing of Test Section	81
11	Photograph of Experimental Apparatus	82
12	Photograph of Test Section	83
13	Condensation Coefficient σ Versus Pressure P_s for Steady-State Evaporation Experiment	84
14	Condensation Coefficient σ Versus Pressure P_s for Various Liquid Metals	85
15	U Versus Pressure P_s	86
16	General Kinetic Model of the Interface	87
17	Illustration of the Relationship Between δT_k and δT_c	88

LIST OF SYMBOLS

Symbols

f	velocity distribution function - see Equation (A-1)
h	specific enthalpy
h_{fg}	$h_{fg} \equiv h_g - h_f$
h'_{fg}	see Equation (I-5-5a)
h_{Hg}	liquid depth
J_i	mass flux
J_m	momentum flux
J_s	$J_s \equiv P / \sqrt{2\pi RT}$
J_u	energy flux
K	transport coefficient
k	thermal conductivity
L_{ii}	transport coefficient
L_k	transport coefficient
P	pressure
q^*	see Equation (I-5-5a)
q/A	heat transfer per unit area per unit time
Q	fluxes over and above that calculated from integrating half maxwellian velocity distributions - see Section VII
R	gas constant
T	temperature
U	see Equation (V-1)
X	distance
α	energy accommodation coefficient
ΔP	$\Delta P \equiv P_g - P_s (T_{fi})$

Symbols

δT	$\delta T \equiv T_{gi} - T_{fi}$
δT_k	δT as defined by Kennard
Γ	discussed under Equation (I-3-1)
γ	specific heat ratio c_p/c_v
σ	condensation or evaporation coefficient
ω	estimated error in experimental quantity

Subscripts

avg	average
f	liquid
g	vapor
i	liquid-vapor interface
max	maximum
min	minimum
NI	nickel
s	saturation condition
ss	steady state
w	wall
1, 2, 3, 4	see Figure 2
α', α''	see Figure 16

Superscript

E	equilibrium situation
---	-----------------------

I. INTRODUCTION

I-1. Nusselt's Analysis of Condensation

The present work is concerned with the liquid-vapor phase change process. Consider a saturated condensable vapor at the temperature T_∞ condensing on a vertical wall at the temperature T_w as is illustrated in Figure 1. This problem was first formulated by Nusselt⁽¹⁾ who assumed, among other things, a temperature distribution as is shown in Figure 1. With the assumed uniform vapor temperature, the energy flux in the vapor J_u is $h_g J_i$. His analysis was later modified to take into account momentum effects in the liquid, shear stress at the liquid-vapor interface, and non-linearity in the condensate film. Although experiments have substantially borne out the theoretical predictions for non-liquid metals, for liquid metals, heat transfer rates are found to be five to thirty times lower than that predicted.⁽²⁾ It follows that some additional resistance to heat transfer is present.

I-2. Resistance of the Liquid-Vapor Interface

A review of the literature as presented by Kroger⁽²⁾ leads to the conclusion that the major resistance to heat transfer during condensation of liquid metals is to be found at the liquid-vapor interface.

The liquid-vapor interface resistance appears as a temperature difference δT between the bulk flow region of the condensate liquid film and the bulk flow region of the vapor. This temperature difference arises from the fact that when material passes from one phase to another at a net finite rate, there is a finite nonequilibrium region at the interface. In this nonequilibrium region, thermodynamic properties such as temperature and chemical potential lose their meaning, as also does the

Fourier heat conduction law along with other continuum equations. We should not expect a finite rate of mass or energy to pass through this region without a corresponding change in temperature and chemical potential. Subsequently, we shall speak of these changes as discontinuities (e.g. δT) realizing, however, that they really result from a gap in the temperature and chemical potential profiles.

1-3. Schrage's Kinetic Analysis of the Phase Change

To account for this additional resistance, Sukhatme and Rohsenow⁽³⁾ and Kroger⁽²⁾ incorporated into Nusselt's analysis an equation for the rate of phase change given by Schrage.⁽⁴⁾

Schrage considers a control surface α' on the vapor side of the liquid-vapor interface as is illustrated in Figure 2. He then assumes that the velocity distribution of the incident molecules crossing α' to the left is that of a half maxwellian with a superimposed bulk velocity V and is characterized by the temperature T_g and the pressure P_g . This distribution is the same as that of the vapor molecules far from the interface which have a velocity toward the interface. For such a distribution to persist right up to the interface, as is assumed by Schrage, would require a collisionless region on the vapor side of the interface. The molecules crossing α' to the right are considered to be composed of two parts the first of which consists of molecules emitted from the liquid. The emission process is assumed to depend only on the temperature of the liquid surface. The expression for the rate of emission is obtained by considering an equilibrium situation where the incident distribution is half maxwellian at the temperature of the liquid surface T_{fi} and the corresponding saturation pressure $P_g(T_{fi})$, (see Appendix A).

The second part crossing α' to the right consists of those incident molecules which are reflected from the interface. This second part is related to the incident flux by way of the condensation coefficient ∇ which is defined as the fraction of incident molecules which condense. On integrating the assumed velocity distributions and using the definition of ∇ , the following equation results for the rate of phase change

$$J_i = - \frac{\nabla}{\sqrt{2\pi R}} \left[\Gamma \frac{P_g}{T_g^{1/2}} - \frac{P_s}{T_{fi}^{1/2}} \right], \quad (I-3-1)$$

where R is the gas constant and Γ accounts for the bulk-flow velocity in the assumed incident distribution. To arrive at Equation (I-3-1), it is necessary to assume that ∇ depends only on the temperature T_{fi} as is discussed in Appendix A. It should be pointed out that Schrage does not require that his assumed velocity distributions satisfy the momentum equation or Onsager's reciprocal relation. This point is discussed in Section VII-I.

For low rates of phase change where

$$\frac{\delta P}{P} \equiv \frac{P_{gi} - P_s}{P_{gi}} \approx \frac{P_{gi} - P_s}{P_s} \ll 1, \quad (I-3-2)$$

$$\frac{\delta T}{T} \equiv \frac{T_{gi} - T_{fi}}{T_{gi}} \approx \frac{T_{gi} - T_{fi}}{T_{fi}} \ll 1, \quad (I-3-3)$$

and

$$\Gamma \approx 1 - \frac{J_i}{P_s} \sqrt{\frac{\pi R T_{fi}}{2}}, \quad (I-3-4)$$

Equation (I-3-1) becomes

$$J_i = \frac{2\sigma}{2-\sigma} \frac{P}{\sqrt{2\pi RT}} \left(\frac{\delta T}{2T} - \frac{\delta P}{P} \right) . \quad (I-3-5)$$

It should be pointed out that δP is not an actual pressure change realized during the phase change but a quantity which can be calculated from the actual pressure at the interface P_{gi} and the temperature of the liquid side of the interface T_{fi} .

I-4. Incorporation of Schrage's Kinetic Analysis into the Condensation Problem

The usual way⁽³⁾ of incorporating Schrage's analysis into the condensation problem is to model the process as is shown in Figure 3. From this figure we see that for the same T_∞ and T_w , there is a lower heat flux at the wall due to the δT at the liquid-vapor interface. Again, as in Nusselt's analysis the temperature profile in the vapor is assumed uniform, and the energy flux J_u is thus given by $h_g J_i$. Using the assumed temperature $T_{gi} = T_\infty$, experimental values of heat flux, T_w , and also Nusselt's theory to arrive at T_{fi} , and therefore $P_s(T_{fi})$, one may calculate values of σ from Schrage's Equation (I-3-1).

I-5. Linear Irreversible Thermodynamic Analysis of the Phase Change

Recently Bornhorst⁽⁵⁾ presented an analysis of the phase change problem which is based on the concepts of linear irreversible thermodynamics. The thermodynamic analysis requires no assumption about molecular details as is required in the kinetic analysis. Bornhorst's solution contains an equation for the rate of phase change which is similar in form to the linearized version of Schrage's Equation (I-3-5).

$$J_i = RL_{ii} \left[\frac{2h_{fg}}{RT} \left(\frac{K}{K+1} \right) \frac{\delta T}{2T} - \frac{\delta P}{P} \right] \quad (I-5-1)$$

In addition Bornhorst's analysis yields an equation for the energy flux J_u .

$$J_u = \left[h_{gi} - \left(\frac{K}{K+1} \right) h_{fg} \right] J_i - \frac{L_k}{T} \frac{\delta T}{T} \quad (I-5-2)$$

where h_{gi} and h_{fi} are the enthalpy of the vapor and liquid, respectively, at the interface and $h_{fg} \equiv h_{gi} - h_{fi}$. Appearing in Equations (I-5-1) and (I-5-2) are the thermodynamic properties L_{ii} , L_k , and K which are called transport coefficients and which must be determined from experiment. The thermodynamics of irreversible processes is presently restricted to processes which are not inherently non-linear and in which terms containing $(\delta T/T)^2$ and $(\delta P/P)^2$ are negligible compared to terms containing $(\delta T/T)$ and $(\delta P/P)$ (see Reference 6.)

Meaning of the Transport Coefficient L_{ii}

By considering an isothermal experiment in which $\delta T = 0$, we see from Equation (I-5-1) that L_{ii} is given by

$$L_{ii} = - \frac{(J_i)_{\delta T=0} P}{R (\delta P)_{\delta T=0}} \quad (I-5-3)$$

The relation between L_{ii} and the condensation coefficient σ appearing in Schrage's analysis is obtained by comparing Equations (I-3-5) and (I-5-1) when $\delta T = 0$. The result is

$$L_{ii} = \frac{2\sigma}{2-\sigma} \frac{P}{R \sqrt{2\pi RT}} \quad (I-5-4)$$

Meaning of the Transport Coefficient L_k

For an experiment in which there is a steady heat transfer J_u through a system composed of a vapor coexisting with its liquid phase and in which there is no net change of phase ($J_i = 0$) as is illustrated in Figure 4, we see from Equation (I-5-2) that the transport coefficient L_k is given by

$$L_k = - \frac{(J_u)_{J_i=0}}{(\delta T)_{J_i=0}} T^2 .$$

From this equation we see that L_k is a measure of the conductance of the interface to heat transfer. On a microscopic scale L_k is related to the energy accommodation coefficient α by way of the temperature jump analysis of Kennard. (7, 5)

$$L_k = \left(\frac{\gamma + 1}{\gamma - 1} \right) \sqrt{\frac{R}{2\pi}} T^{3/2} P \left(\frac{\alpha}{2 - \alpha} \right) , \quad (I-5-5)$$

where γ is the ratio of specific heats of the gas phase. The energy accommodation coefficient should be very close to unity for a liquid-vapor interface, especially for a fluid having a high molecular weight. (8)

Meaning of the Transport Coefficient K

In order to illustrate the meaning of the transport coefficient K , we shall again consider the isothermal experiment where $\delta T = 0$. A sketch of the experiment is given in Figure 5. Reservoir 1 supplies energy to the liquid in the form of a heat transfer which results in evaporation at the liquid-vapor interface. If the walls bounding the vapor were adiabatic, the situation would be one of steady-state evaporation, which

is discussed later in Section II, and there would be a δT at the interface with the vapor being at a uniform temperature T_g lower than T_{fi} . In order to maintain zero δT , reservoir 2 is employed. We thus see that in order to maintain zero δT there is a heat transfer in both the liquid and vapor phase, and all of the heat necessary for evaporation does not come from only the liquid side of the interface. The basic definition of K , as given by Bornhorst,⁽⁵⁾ is the ratio of the heat transfer from reservoir 2 to that from reservoir 1.

The reason why some of the heat must come from the vapor side is illustrated by considering the latent heat of evaporation to be composed of two parts

$$h_{fg} = h_{fg}' + q^* \quad . \quad (I-5-5a)$$

The first part h_{fg}' is that energy necessary to separate or emit the molecules from the liquid. It is expected that most of this energy will come from the liquid side. Immediately after emission the molecules will have some velocity distribution associated with them which will not necessarily be the same as that in the bulk flow region of the vapor. In order to attain the distribution in the bulk region, there will, in general, be the additional energy transfer q^* . This energy transfer is a result of the redistribution of the molecular velocities, and part of it is expected to come from the vapor. In Appendix C it is shown that if a half maxwellian velocity distribution is assumed for the emitted and incident molecules, the energy transfer q^* is given by $\frac{1}{2} RT$.

The meaning of K can also be found by considering Equation (I-5-2) for the special case of zero δT

$$(J_u)_{\delta T=0} = h_{gi} (J_i)_{\delta T=0} - \left(\frac{K}{K+1}\right) h_{fg} (J_i)_{\delta T=0} \quad (I-5-6)$$

From Equation (I-5-6) we see that K is a measure of how the heat of vaporization splits at the interface for zero δT ; that is, $\frac{K}{K+1}$ is the fraction of the heat $h_{fg} J_i$ necessary for evaporation which is transferred to the interface from the vapor side while $(1 - \frac{K}{K+1})$ is that which is transferred from the liquid side when δT is zero. When K is zero all of the heat is from the liquid side.

When δT is non-zero, there is, in addition to the above-mentioned heat transfer, another contribution to the heat transfer in the vapor. This is due to the conductance of the interface, and the magnitude of this additional heat transfer is given by $-\frac{L_k}{T} \frac{\delta T}{T}$. Thus for the general case the net heat transfer in the vapor at the interface is given by

$$(q/A)_g = -\frac{K}{K+1} h_{fg} J_i - \frac{L_k}{T} \frac{\delta T}{T} \quad (I-5-7)$$

This equation follows directly from Equation (I-5-2) by expressing J_u as the sum of the enthalpy flux plus the heat transfer.

Another interpretation of K is obtained by considering Equation (I-5-1) for the special case of no flow as is illustrated in Figure 4. For such a situation Equation (I-5-1) reduces to

$$\frac{K}{K+1} = \frac{RT}{2 h_{fg}} \left(\frac{\delta P/P}{\delta T/2T}\right)_{J_i=0} \quad (I-5-8)$$

Thus K is a measure of the ratio of δP to δT necessary to maintain zero net phase change when there is a heat transfer across the interface.

I-6. Incorporation of the Thermodynamic Analysis into the Condensation Problem

With the thermodynamic analysis in mind, we see that we are no longer justified in assuming that the temperature in the vapor is uniform during condensation as it is in Figure 3. There will be a gradient in the vapor temperature profile at the interface. Whether the gradient is positive or negative depends on the sign of $(q/A)_g$ in Equation (I-5-7). One possible temperature profile is illustrated in Figure 6. The temperature gradient is found to fall off exponentially with distance from the interface⁽⁵⁾ thus making it very difficult to measure T_{gi} during a condensation experiment.

I-7. Basic Differences Between the Thermodynamic Analyses and Schrage's Theory

In order to perform Schrage's kinetic analysis, it was necessary to assume velocity distributions for the vapor molecules near the interface. No such assumptions concerning molecular detail are needed for the thermodynamic analysis. The kinetic derivation based itself on the definition of the condensation coefficient. No such definition is required in the thermodynamic analysis, and the transport coefficients appearing in the thermodynamic result are thermodynamic properties within the linear assumptions. Also, the irreversible analysis requires at the very beginning that the solution obtained satisfies the general laws of thermodynamics and in particular the second law. This is assured by following the formalism of irreversible thermodynamics which essentially results in the Onsager reciprocal law. Schrage does not require that his velocity distributions satisfy these laws.

The limitations of the thermodynamic analysis have been mentioned in Section I-5. It should be noted that the restriction that $(\delta T/T)^2 \ll (\delta T/T)$ in going from Equation (I-3-1) to (I-3-5) is not the same as the restriction regarding $(\delta T/T)$ and $(\delta T/T)^2$ terms in the thermodynamic analysis.

I-8. Present Investigation

The purpose of this investigation is to measure the transport coefficients K and L_{ii} (or ∇). This is accomplished by performing the experiment described in Section II and by assuming the coefficient L_k . This assumption is discussed in Section V-1. In the light of the experimental results a kinetic model of the phase change is then developed which is consistent with the conservation laws, Onsager's reciprocal law, and experiment.

The experiment is unique in that this is the first time that the transport coefficient K has been measured. In addition to being the first attempt at measuring K , this is the first time that the condensation coefficient ∇ has been measured during evaporation of a liquid metal, namely, mercury, other than for evaporation into a vacuum. One of the major problems in any experiment involving phase change is contamination. Contamination results in an added resistance to phase change. During condensation most of the contamination is attributed to noncondensable gases in the vapor⁽²⁾ while during evaporation, it is attributed to surface active agents in the liquid. The results of this work will illustrate the relative importance of the two.

II. EXPERIMENTAL METHOD

The no-flow experiment, though conceptually simple, is difficult to perform in practice. The result for L_k given in Equation (I-5-5) predicts that the temperature discontinuity at the interface is equal to twice the temperature difference across a mean free path in the vapor. Thus, to maintain a temperature discontinuity δT of 1 °F during no-flow steady-state experiments, carried out at the pressure levels used in condensation experiments, (2,3,9) would require vapor temperature gradients of the order of 1,000 to 100,000 °F/inch. In addition to the problem of measuring such a temperature distribution, there is the problem of insuring that J_i is zero everywhere. For J_i to be zero at a particular point, it is necessary that there be a balance between the local driving forces δP and δT as can be seen from Equation (I-5-1). Any foreign body, such as a probe in the vapor or the containing walls of the apparatus, will disturb the temperature distribution, thereby destroying the balance between δP and δT with resulting rates of phase change J_i .

The isothermal experiment is also difficult to perform in practice. To insure isothermal conditions, it would be necessary to measure the temperature distribution in the vapor. This is a difficult task because of the errors introduced by conduction along probes and radiation between the probe and its surroundings. Controlling $\delta T = 0$ is also a difficult task.

In both the isothermal and the no-flow experiments, the problem of measuring a non-uniform temperature distribution in a vapor arises. For this reason an experiment has been devised in which the vapor temperature is uniform. We shall call this experiment the steady-state evaporation experiment and proceed to define it.

II-1. Steady-State Evaporation Experiment

A steady-state evaporation experiment, as is illustrated in Figure 7, is one in which liquid changes to the vapor phase at a constant rate by evaporation at the liquid-vapor interface with the absence of boiling and in which the heat transfer necessary for evaporation is all from the liquid side of the interface. There is no heat transfer to the vapor. For such a situation the vapor temperature far from the interface will eventually reach some uniform value. By first-law consideration, it can be seen as follows that the vapor temperature will be uniform right up to the interface. Assume that the vapor temperature is uniform far from the surface and then starts to decrease near the interface as is illustrated in Figure 8. We see that the enthalpy flux leaving the control volume is higher than that entering. For this to happen it is necessary that there be a heat transfer into the control volume; however, for the assumed temperature distribution, the heat transfer is out of the control volume. We conclude, therefore, that the temperature cannot decrease as shown. By using the same argument one can also show that the temperature cannot increase.

II-2. Equations for Steady-State Evaporation

For steady-state evaporation we have seen that the heat transfer in the vapor at the interface is zero and that the energy flux is thus given by

$$(J_u)_{ss} = h_g (J_i)_{ss} \quad (II-1-1)$$

where the subscript ss denotes steady-state evaporation. Moreover, the heat transfer contribution in the vapor due to the splitting of $h_{fg} J_i$,

namely, $\frac{K}{K+1} h_{fg} J_i$, is balanced by that contribution due to the conductance of the interface, namely, $\frac{L_k}{T} \frac{\delta T}{T}$. In other words $(q/A)_g$ is zero in Equation (I-5-7); this results in an expression for K

$$\frac{K}{K+1} = - \frac{1}{h_{fg}} \frac{L_k}{T^2} \left(\frac{\delta T}{J_i} \right)_{ss} . \quad (\text{II-1-2})$$

The equation for the rate of phase change for steady-state evaporation, from Equation (I-5-1) is

$$(J_i)_{ss} = L_{ii} R \left[\frac{2h_{fg}}{RT} \left(\frac{K}{K+1} \right) \frac{(\delta T)_{ss}}{2T} - \frac{(\delta P)_{ss}}{P} \right] . \quad (\text{II-1-3})$$

Thus using the measured quantities T_{gi} , T_{fi} , P_g , and $(J_i)_{ss}$ and taking L_k from Equation (I-5-5), one can determine K and L_{ii} (or ∇) from Equations (II-1-2) and (II-1-3) (or (I-3-5)).

III. EXPERIMENTAL APPARATUS

A flow diagram of the steady-state evaporation experiment is sketched in Figure 9. Figure 10 contains a drawing of the test section, and photographs of the experimental apparatus are illustrated in Figures 11 and 12. A thin layer of liquid mercury on the nickel block is evaporated, the necessary heat being supplied by electrical heaters placed in the nickel. The temperature distribution in the nickel block is measured with thermocouples and extrapolated through the liquid layer to determine the temperature on the liquid side of the interface T_{fi} . To extrapolate it is necessary to know the depth of the liquid layer. The liquid depth is determined by measuring the displacement of a needle-like probe when it is moved from the solid nickel surface to the liquid surface by means of micrometer heads.

Nickel was chosen as the material for the heating block because mercury wets nickel. It is necessary to have a wettable surface if a thin film of liquid is to be realized; also the wetting minimizes any contact resistance which may exist at the solid-liquid interface.

It is desirable to have a thin layer of liquid so that any error in the extrapolation which may result from a non-linear temperature profile in the liquid will be minimized. Also a thin layer minimizes the possibility of convection. Finally, a thin layer of liquid will minimize the possibility of having active nucleation sites for boiling by reducing the superheat at the nickel surface.

The depth of the liquid layer is controlled by adjusting the slope of the nickel block, the height of the weir placed at the downstream end of the nickel block, and the flow rate.

It should be noted that there is a means of having a liquid flow rate into the test section which is greater than that evaporated. This excess flow rate is termed the overflow. The reason for incorporating the overflow is to provide some means of keeping the liquid surface clean.

The temperature in the vapor T_g , which must be uniform to satisfy the first law requirements for steady-state evaporation, is measured by thermocouples at various locations and orientations as is shown in Figure 12.

The thermocouples are copper-constantan enclosed in stainless steel sheaths. They were calibrated against a standard platinum resistance thermometer.

The rate of evaporation, J_1 , is determined from the heat transfer to the liquid, which is given by the temperature gradient and conductivity in the nickel and the latent heat h_{fg} . A means of checking this is by taking the difference between the supply and overflow rate of liquid mercury.

The pressure in the test section P_g is measured by a manometer. One leg of the manometer is connected to a plenum chamber which is in turn kept at zero pressure by a vacuum pump. The other leg of the manometer is connected to the test section. Since room temperature is less than the saturation temperature in the test section, any mercury vapor in the manometer lines would tend to condense. Eventually condensate would form in the manometer. To eliminate this problem, the manometer line is filled with argon. The mercury vapor thus has to diffuse through the argon before reaching the manometer. The line is also placed at an angle to the horizontal so that any condensate which forms will

fall back into the test section. During testing no condensate was observed to form in the pressure tap line.

The remainder of the system consists of an annular counterflow water-cooled condenser, a condensate collector tank, an ice trap to condense any mercury vapor which gets past the condenser, a mercury filter to absorb any mercury vapor which gets past the ice trap, and a vacuum pump which exhausts into the laboratory exhaust system. Since the system pressure will be below atmospheric, any leakage will be into the system, thus minimizing any health hazard from the toxic mercury vapor.

IV. EXPERIMENTAL OPERATING PROCEDURE

First, all parts were cleaned in hydrochloric acid, trichlorethylene, and acetone. The system was then tested for leaks, and then triply distilled mercury was introduced in the liquid supply tank.

The nickel heating block was then covered with mercury and kept at a temperature of 500 °F for two days to obtain the desired condition of a wetted surface. Subsequently, it was found that a small region of the nickel block near the weir and the nickel weir itself did not have wetted surfaces. This was overcome by rubbing the unwetted portion of the surface with hydrochloric acid. To preserve the wetting condition, the surfaces are kept covered with liquid. Should the surface become dry and then non-wettable, it is necessary to clean the unwetted surface with hydrochloric acid.

To achieve a condition of steady-state evaporation, the following steps are followed:

1. The portion of the system bounded by the dotted lines in Figure 9 is heated to the desired temperature by heating tapes wrapped around the system. The saturation pressure corresponding to this temperature determines the pressure level at which the system is maintained during the test.
2. The condenser cooling water is turned on, and ice is supplied to the ice trap and thermocouple reference junction.
3. With the system-pressure control valve 1 open, vacuum pump A is used to lower the system pressure below the desired operating value.
4. Valve 1 is then closed. If necessary the vacuum pump valve 2 is left open a small amount to purge any gases which may leak into the system during the test.

5. The heaters in the nickel block are turned on. Evaporation will commence resulting in an increase in pressure. Valve 1 is then opened accordingly to maintain the desired pressure.

It was found that the temperature of the horizontal thermocouple probe in the vapor was sensitive to the pressure level. When the pressure was decreased, the temperature of the horizontal probe decreased. The vertical probes, however, were found to be relatively insensitive to the pressure level. For a fixed amount of input heater power, and thus a fixed evaporation rate, the temperature of the liquid surface will decrease when the pressure is decreased because the fixed flow rate requires a fixed δP as can be seen from Equation (I-5-1). This results in a decrease in the temperature of the vapor. At the same time, the temperature of the bounding walls will not decrease as rapidly because of thermal inertia. We thus conclude that the temperature of the horizontal probe is closer to that of the vapor temperature, and the temperature of the vertical probe is closer to that of the bounding walls. This is exactly what is expected from considerations of the respective orientations of the probes. Equality of temperature between the vapor and the bounding walls was assumed when the probes in the vapor were all at the same temperature. To verify this, a test was performed with a radiation shield, consisting of two concentric cylinders, placed around the vertical probes. A thermocouple was also placed in the wall. All the thermocouples were at the same temperature during the test, and the results of this test were in accord with those obtained previously.

6. The weir and supply flow rates are adjusted such as to give the desired liquid level. The overflow rate varied from 1.5 to 3.0 times the evaporation rate J_1 . To obtain a reference level for the micrometer heads at the operating condition, it is necessary to know when the points of the depth probes contact the solid nickel surface while there is mercury on the surface. There is enough play between the O-ring sealed-shaft cylinder arrangement to move the tips of the probes horizontally. Contact with the solid surface is indicated when the probe tips are no longer free to move horizontally.

It takes about one to two hours to obtain the testing condition. After a test the mercury is collected from the overflow and condensate collector tanks. If necessary, it is then put in an oxidizer which oxidizes impurities in the mercury. The mercury is finally filtered before being returned to the supply tank.

V. EXPERIMENTAL DETERMINATION OF TRANSPORT COEFFICIENTS

V-1. Relationships Between the Transport Coefficients and Measurable Quantities

In place of the transport coefficient K , it is more convenient to express the experimental results in terms of the coefficient U which is related to K by the following definition

$$U \equiv \frac{K}{K + 1} \frac{2 h_{fg}}{RT} \quad . \quad (V-1-1)$$

For the steady-state evaporation experiment, the expression for U is obtained by combining Equations (V-1-1) and (II-1-2)

$$U = - \frac{2L_k}{RT^3} \left(\frac{\delta T}{J_{i ss}} \right) \quad . \quad (V-1-2)$$

The recent work of Teagan⁽¹⁶⁾ indicates that the temperature jump analysis of Kennard,⁽⁷⁾ which is based on a model of the gas kinetics at a solid-vapor interface and which was used to arrive at the expression for L_k (Equation I-5-5), is a good approximation for a solid-vapor interface. The kinetics of the gas adjacent to a liquid-vapor interface during no-flow is expected to be the same as that adjacent to a solid-vapor interface. What may differ is the mechanism by which accommodation or transfer of energy from the vapor molecules to the interface takes place. This, however, does not enter into the Kennard analysis. Since the energy accommodation coefficient α is expected to be unity for a liquid-vapor interface, it is not unreasonable to assume that L_k is given by Equation (I-5-5) with $\alpha = 1$. The reason for expecting α to be unity is because

the condensation coefficient σ is found to be close to unity. This means that most of the molecules striking the liquid condense. Thus most of the molecules leaving the liquid surface will be those that are emitted, and the emitted distribution should have a temperature equal to that of the liquid. In addition, the small fraction $(1 - \sigma)$ of molecules which are "reflected" from the interface should be well accommodated when the molecular weight is as high as that of mercury.

Substitution of Equation (I-5-5) for L_k with $\alpha = 1$ into Equation (V-2) yields the following result for U in terms of measurable quantities:

$$U = - \left(\frac{\gamma + 1}{\gamma - 1} \right) \sqrt{\frac{2}{\pi R}} \frac{P}{T^{3/2}} \left(\frac{\delta T}{J_i} \right)_{ss} \quad (V-1-3)$$

In place of the transport coefficient L_{ii} , the experimental results are expressed in terms of σ as it appears in Schrage's Equation (I-3-5)

$$\frac{2\sigma}{2 - \sigma} = (J_i)_{ss} \frac{\sqrt{2\pi RT}}{P} \left[\frac{(\delta T)_{ss}}{2T} - \frac{(\delta P)_{ss}}{P} \right]^{-1} \quad (V-1-4)$$

The difference between the values of σ calculated from Equation (V-1-4) where the coefficient of $(\delta T)_{ss}/2T$ is taken to be unity compared to the result obtained when the coefficient is taken to be U as it appears in the thermodynamic analysis is negligible. The reason for this is that the term $(\delta T/2T)_{ss}$ is experimentally found to be approximately 1/25 of the $(\delta P/P)_{ss}$ term.

V-2. Necessary Measurements

The quantities needed from the experiment to evaluate the right-hand side of Equations (V-1-3) and (V-1-4) are J_i , T_{fi} , T_{gi} , and P . T_{gi}

and P are measured directly by thermocouples in the vapor and a manometer. To obtain T_{fi} , the liquid interface temperature, it is necessary to extrapolate the temperature measurements made in the nickel heating block. The surface temperature of the nickel interface T_{NI} is obtained by putting a-least-squares straight line fit through the temperatures measured in the region near the surface of the nickel block where the temperature profile is approximately a straight line. The slope of this straight line multiplied by the ratio of the thermal conductivity of the nickel to that of the mercury gives the slope in the liquid. This slope along with the height of the liquid h_{Hg} and T_{NI} yields T_{fi} ,

$$T_{fi} = T_{NI} - \left(\frac{k_{NI}}{k_{Hg}}\right) \left(\frac{\Delta T}{\Delta X}\right)_{NI} h_{Hg} \quad (V-2-1)$$

The quantity

$$(\Delta T)_{ss} = T_{gi} - T_{fi} \quad (V-2-2)$$

can be now calculated as well as

$$(\Delta P)_{ss} = P - P_s(T_{fi}) \quad (V-2-3)$$

where T_{gi} is the temperature of the vapor, P is the system pressure measured by the manometer, and $P_s(T_{fi})$ is the saturation pressure corresponding to the liquid interface temperature. The rate of evaporation $(J_i)_{ss}$ is obtained from

$$(J_i)_{ss} = \frac{k_{NI}}{h_{fg}} \left(\frac{\Delta T}{\Delta X}\right)_{NI} \quad (V-2-4)$$

The saturation pressure data for mercury were taken from Reference 15, the other properties of mercury from Reference 17, and the thermal conductivity of nickel from Reference 18.

The errors due to measurement and in assuming the above relationships between the measurements and the desired physical quantities are discussed in Appendix B .

V-3. Experimental Results

Figure 13 illustrates the values of the coefficient σ obtained from the steady-state evaporation experiment. Included are the error bands resulting from the experimental uncertainties discussed in Appendix B. It should be observed that none of the lower limits of the error bands are above unity. There are three points C, D, and E having low values of σ which are less than 0.4. At the time these points were taken, a film of impurities was observed on the liquid surface. This film would result whenever the overflow region of the nickel heating block did not wet properly. Instead of having the entire surface freely flowing, there would be regions of stagnant surface fluid. At these stagnant regions, a film would develop with time. The film acts as a resistance to the evaporation thereby requiring a large driving force ΔP which results in low values of σ . These three points clearly show the strong influence of the condition of the surface on the coefficient σ . There are four data points having values of $\sigma \approx 0.6$. The impurity film was not observed for these points; however, points F and G were taken during a time in which much difficulty was encountered in preventing the buildup of the film. The remaining points are found to be scattered within their error bands around σ of about 0.9. From this we

conclude that the scatter outside of the experimental uncertainties is due to the absence of a sufficiently free flowing surface.

The values of ∇ , excluding those suspected of being affected by contamination, are shown in Figure 14 along with the condensation results of previous investigations for various liquid metals.

Figure 15 shows the experimental values of U as well as the error bands. The value of U which best fits the data is about 0.27.

The experimental results are tabulated in Table 1.

VI. DISCUSSION OF EXPERIMENTAL RESULTS

VI-1. Concerning the Coefficient σ

Figure 14 shows that the values of the coefficient σ obtained in the present investigation are higher than those previously obtained during the condensation of mercury experiments.^{(3), (9)} In the present study σ was found to decrease when contamination in the form of an impurity film was present. Knudsen⁽²⁰⁾ observed this same effect when he measured σ , from Equation (I-3-1), for evaporation of a mercury droplet into a vacuum. He obtained values of σ much less than unity. He observed, however, that the surface of the droplet was contaminated as it was light brown in color. To eliminate the contamination, he renewed the droplet every fourth second. The resulting values of σ were unity. Volmer and Esterman⁽²¹⁾ also obtained σ equal to unity for the evaporation of mercury into a vacuum by taking precautions to avoid surface contamination.

In the previous condensation experiments, σ was found to decrease when non-condensable gases were intentionally introduced.^{(2), (3)} It is very difficult to remove all traces of noncondensables from an experimental system. Any noncondensables which are present will eventually be transported to the interface by the condensing vapors. A layer of noncondensable gas will thus be formed on the vapor side of the interface. The condensing vapors will then have to diffuse through the noncondensables. This added diffusional resistance results in lower values of σ . The problem of noncondensables is minimized in an evaporation experiment because the vapor will carry the noncondensables away from the interface.

It is suspected, therefore, that the lower values of ∇ obtained from the condensation experiments may be due to contamination. If this is the case, then the true value of ∇ , which occurs in the absence of all contamination, is more easily measured from evaporation experiments.

The value of ∇ obtained from condensation experiments is found to decrease with increasing values of P_g as is illustrated in Figure 14. The results of the present investigation suggest that this may not be the case for evaporation.

VI-2. Concerning the Coefficient K or U

The experimental value of U is found to be 0.27. An extension of Schrage's method of analyzing the phase change process is not in accord as it requires that U be unity. This result is derived in Section VII-2. A more general kinetic model of the phase change process, however, which is developed in Section VII-3, shows that U is not necessarily equal to unity. We shall now proceed to discuss the kinetic analysis of the phase change in the light of the experimental results.

VII. ANALYTICAL CONSIDERATION OF THE KINETICS AND THERMODYNAMICS OF THE INTERFACE

In this section the kinetic analysis of the phase change process is studied. A method of analysis is presented which is consistent with the conservation laws, Onsager's reciprocal law, and experiment.

Before proceeding with the analysis, it is necessary to explain two different methods of describing the kinetics in the vapor adjacent to the interface. In the first method, termed method A, velocity distributions are assigned to the molecules crossing a control surface. The net fluxes of mass, momentum, and energy across the control surface are calculated by integrating the distribution functions. This method thus requires that the velocity distributions employed be exact. This is the method of description used by Schrage.

In the second method, termed method B, we do not attempt to assign the exact distributions; instead we use approximate distributions. In general, the fluxes obtained from integration of these distributions are in error. To account for this error, we allow for additional fluxes of mass, momentum, and energy. We term these additional fluxes Q_i , Q_m , and Q_u . Method B is best explained by considering the familiar situation of a temperature gradient dT/dx in a semiperfect monatomic gas moving at a low Mach number. At a control surface in the gas, we consider the molecules to be described by a Maxwellian distribution with a superimposed bulk flow velocity. Integration of this distribution yields the enthalpy flux $h_g J_i$. The net energy flux is greater than this, however, by the amount

$$Q_u = -k \frac{dT}{dx}$$

where k is the thermal conductivity of the gas. This example illustrates that we do not attempt to guess the exact velocity distribution. Instead we assume an approximate distribution and account for the difference between it and the real distribution by means of a conductivity term.

VII-1. Conservation of Momentum Considerations

Relationship Between the Parameters Defining the Velocity Distribution

In this section the kinetics of the vapor adjacent to the liquid surface is described by method A. Let the velocity distribution of the molecules incident on the liquid surface be denoted by f_2 ; the molecules emitted from the liquid surface, by f_3 ; and the molecules reflected from the surface, by f_4 . Let the distribution functions be half maxwellian characterized by the parameters P_j and T_j

$$f_j = \frac{P_j}{m RT_j (2\pi RT_j)^{3/2}} e^{-\frac{1}{2 RT_j} (u^2 + v^2 + w^2)} , \quad (\text{VII-1-1})$$

where m is the weight of a molecule, u is the molecular velocity perpendicular to the interface, and v and w are the mutually perpendicular velocities in a plane perpendicular to u (Figure 16). By a half maxwellian it is meant that for the distribution f_2 , $-\infty \leq u \leq 0$ and for f_3 and f_4 , $0 \leq u \leq \infty$. For all distributions $-\infty \leq v \leq \infty$ and $-\infty \leq w \leq \infty$. Assume that P_3 and T_3 are given by

$$T_3 = T_{fi}$$

$$P_3 = P_s(T_{fi}) , \quad (\text{VII-1-2})$$

With the above assumptions and by invoking the conservation of momentum equation, we shall proceed to find a relationship between the parameters P_j and T_j .

Let J_{mj} represent the momentum flux of the distribution f_j . The conservation of momentum requires that

$$J_{m2} + J_{m3} + J_{m4} = J_{m1} \quad (\text{VII-1-3})$$

where the subscript 1 denotes the bulk flow region of the vapor. For a half maxwellian velocity distribution, it can be shown that

$$J_{mj} = J_{ij} \sqrt{\frac{\pi RT_j}{2}} \quad (\text{VII-1-4})$$

and

$$J_{ij} = \frac{P_j}{\sqrt{2 \pi RT_j}} \quad (\text{VII-1-5})$$

The temperature T_4 of the reflected velocity distribution is related to the temperature of the incident distribution T_2 and the liquid temperature T_{fi} by the energy accommodation coefficient

$$\frac{T_4}{T_2} = (1 - \alpha) + \alpha \left(\frac{T_{fi}}{T_2} \right) \quad (\text{VII-1-6})$$

Substituting (VII-1-4), (VII-1-5), and (VII-1-6) into (VII-1-3) and using ∇ to relate J_{i4} to J_{i2}

$$J_{i4} = (1 - \nabla) J_{i2} \quad (\text{VII-1-7})$$

the following is obtained

$$\frac{1}{2} P_2 + \frac{\sigma}{2} P_s + \frac{1}{2} (1 - \sigma) P_2 \left[(1 - \alpha) + \alpha \left(\frac{T_{fi}}{T_2} \right) \right]^{1/2} = J_{ml} \quad (\text{VII-1-8})$$

The quantities δP^* and δT^* are defined as

$$\delta P^* = P_2 - P_s \quad (\text{VII-1-9})$$

$$\delta T^* = T_2 - T_s \quad (\text{VII-1-10})$$

For situations where a linear analysis is valid, that is where terms such as

$$\left(\frac{\delta P}{P} \right)^2 \ll \left(\frac{\delta P}{P} \right) \quad (\text{VII-1-11})$$

and

$$\left(\frac{\delta P^*}{P} \right) \left(\frac{\delta P}{P} \right) \ll \left(\frac{\delta P}{P} \right) \quad (\text{VII-1-12})$$

J_{ml} is given by

$$J_{ml} = P_g \quad (\text{VII-1-13})$$

Also Equation (VII-1-8) reduces to

$$\frac{\delta P^*}{P} = \frac{2}{2 - \sigma} \frac{\delta P}{P} - \left(\frac{\sigma - 1}{2 - \sigma} \right) \alpha \frac{\delta T^*}{2T} \quad (\text{VII-1-14})$$

Experimental values of σ equal to unity have been observed, and for such a case Equation (VII-1-14) reduces to

$$\frac{\delta P^*}{P} = 2 \frac{\delta P}{P} \quad (\text{VII-1-15})$$

Momentum Considerations in Schrage's Model

We shall now proceed to show that the velocity distributions assumed by Schrage do not, in general, satisfy the momentum equation. Schrage incorporates a bulk velocity U in the distribution f_2 . When $J_1 = 0$ the bulk velocity U is also zero, and his distributions are all half maxwellian. Equation (VII-1-15) must, therefore, be satisfied. This requires that

$$P_2 = P_g + \delta P . \quad (\text{VII-1-16})$$

Schrage, however, assigns the pressure P_g to the distribution f_2 .

VII-2. Use of Half Maxwellian Velocity Distributions to Completely Describe the Interface

In this section method A is used to describe the kinetics of the interface. The velocity distributions used in this section are the same as those of Section VII-1. The parameters T_2 and P_2 are determined by requiring the conservation laws and the Onsager relation to be satisfied. For simplicity, and without loss of generality, ∇ is taken to be unity. Thus there are no reflected molecules (Figure 16). The linear assumptions of Equations (VII-1-11 and 12) are made. It will be shown that this method of describing the interface in terms of half maxwellian velocity distributions yields a solution which is not in accord with experiment.

Conservation of Momentum

Since the distribution functions are assumed to be half maxwellian, the results of Section VII-1 may be used. For $\nabla = 1$ Equation (VII-1-13) requires that

$$P_2 = P_s + \alpha(\delta P) . \quad (\text{VII-2-1})$$

Conservation of Energy

Let J_{uj} represent the energy flux of the distribution function f_j .
The conservation of energy applied to Figure 16 requires that

$$J_{u3} - J_{u2} = J_{u1} \quad (\text{VII-2-2})$$

For a half maxwellian distribution, the energy flux is given by

$$J_{uj} = 2 RT_j J_{ij} \quad (\text{VII-2-3})$$

The energy flux J_{u1} in the bulk-flow region of the vapor is given
by

$$J_{u1} = h_g J_i - (q/A)_g \quad (\text{VII-2-4})$$

On using

$$h_g = \frac{5}{2} RT_g \quad (\text{VII-2-5})$$

Equation (VII-2-4) becomes

$$J_{u1} = \frac{5}{2} RT_g J_i - (q/A)_g \quad (\text{VII-2-6})$$

Substitution of Equations (VII-2-6) and (VII-2-3) into Equation (VII-2-2)
yields

$$2 RT_{f1} J_{i3} - 2 RT_2 J_{i2} = \frac{5}{2} RT_g J_i - (q/A)_g \quad (\text{VII-2-7})$$

The expression for the heat transfer in the vapor in terms of the trans-
port coefficients K and L_k is given by Equation (I-5-7).

$$(q/A)_g = \frac{K}{K+1} h_{fg} J_i - L_k \delta T_k \frac{1}{T^2} \quad (\text{VII-2-8})$$

By using Equations (VII-2-7) and (VII-2-8), an expression relating T_2 to J_i and δT_k may be obtained

$$\frac{\Delta T_2}{2T} = \frac{\delta T_k}{T} - \frac{(1-U)}{8} \frac{J_i}{J_s} \quad , \quad (\text{VII-2-9})$$

where ΔT_2 is related to T_2 by

$$\Delta T_2 = T_2 - T_{fi} \quad , \quad (\text{VII-2-10})$$

and where

$$U \equiv \frac{K}{K+1} \frac{2 h_{fg}}{RT} \quad (\text{VII-2-11})$$

is a property which is determined from the steady-state evaporation experiment (Equation (V-1-3)).

Kinetic Expression for J_i

The conservation of mass as applied to Figure 16 requires that

$$J_i = J_{i3} - J_{i2} \quad (\text{VII-2-12})$$

which may be rewritten as

$$\frac{J_i}{J_s} = -2 \frac{\delta P}{P} + \frac{\Delta T_2}{2T} \quad . \quad (\text{VII-2-13})$$

This is accomplished by substituting Equation (VII-1-5) for J_{ij} and replacing T_2 by ΔT_2 . On using Equation (VII-2-9) to eliminate ΔT_2 from (VII-2-13), the following is obtained

$$J_i = J_s \frac{16}{9-U} \left[-\frac{\delta P}{P} + \frac{\delta T_k}{2T} \right] \quad . \quad (\text{VII-2-14})$$

Thermodynamic Expression for J_i

The thermodynamic Equation (I-5-1) for J_i may be rewritten in terms of U as

$$J_i = RL_{ii} \left[-\frac{\delta P}{P} + U \frac{\delta T_k}{2T} \right] \quad (VII-2-15)$$

The coefficient RL_{ii} resulting from the above kinetic model is found by considering the special case when $\delta T_k = 0$.

$$RL_{ii} = J_s \frac{16}{9 - U} \quad (VII-2-16)$$

Discussion of the Analysis

If the above analysis is to be consistent, then the value of U must be unity as can be readily seen by comparing the coefficients of $\frac{\delta T_k}{2T}$ in Equations (VII-2-14) and (VII-2-15). This analysis is thus not general enough to allow for the value of U not equal to unity as has been observed in the steady-state evaporation experiment. Conversely, if the experimentally determined values of U other than unity are correct, then the above method of modeling the interface is not correct. In summary we conclude that the interface kinetics cannot be modeled with half maxwellian velocity distributions if the pressure and temperature of the emitted distribution f_3 are assumed to be T_{fi} and $P_s(T_{fi})$.

It is possible, however, to model the interface with half maxwellian distributions if in addition to allowing P_2 and T_2 to be free parameters, the pressure P_3 is also allowed to be a free parameter (different than P_s). When this is done the experimental results require that P_2 be greater than P_s . This requires that the rate of emission during evaporation be greater than that at equilibrium. This solution is rejected since we

expect the emitted flux to be less for nonequilibrium conditions than for equilibrium conditions for the following reason: At equilibrium molecules emitted from the liquid are replenished from the vapor. During nonequilibrium evaporation the replenishment rate is less. This results in a decrease in concentration of molecules capable of being emitted. Thus, if anything, the emission rate is expected to be lower.

VII-3. Improved Method of Modeling the Interface

In this section method B is used to describe the kinetics in the vapor adjacent to the interface. The net flux across α' in Figure 16 is given by the superimposed fluxes $Q_{\alpha'}$, in addition to that calculated from integrating the distribution functions f_2 , f_3 , and f_4 . The basic assumption in this analysis is that by altering the boundary conditions $Q_{\alpha'}$, can be forced to be zero and that for this condition the distributions f_2 , f_3 , and f_4 are half maxwellian at the common temperature T_{fi} . The parameter P_3 is taken to be P_s , and P_2 is determined by requiring that the momentum equation be satisfied. In the following analysis the subscript $Q_{\alpha'} = 0$ is used to denote this condition. As before, all equations will be linearized.

At the $Q_{\alpha'} = 0$ condition the mass flux $(J_i)_{Q_{\alpha'}=0}$ can be calculated from kinetics since, consistent with the above assumptions, the distribution functions are exactly half maxwellian at this condition. At any other condition ($Q_{\alpha'} \neq 0$), we cannot calculate the mass flux $(J_i)_{Q_{\alpha'} \neq 0}$ because the distribution functions will be perturbed to allow for the $Q_{\alpha'}$. The general relationship for the mass flux may be determined, however, by employing the Onsager reciprocal law. In essence, through the formalism of irreversible thermodynamics, this law relates the effect of

the Q perturbation on the mass flux to the Q perturbation on the energy flux. The condition that must be satisfied to have $Q_{\alpha,} = 0$ is related to the experimentally measured quantities as is shown below.

Conservation of Momentum

For the special case of $Q_{\alpha,} = 0$, the momentum equation (VII-1-12) requires that

$$(P_2)_{Q_{\alpha,}=0} = P_s + \frac{2}{2-\sigma} (\delta P)_{Q_{\alpha,}=0} \quad . \quad (VII-3-1)$$

Kinetic Expression for $(J_i)_{Q_{\alpha,}=0}$

The continuity equation requires that

$$J_i = J_{i3} + J_{i4} - J_{i2} \quad , \quad (VII-3-2)$$

and for the assumed distributions, this reduces to

$$\left(\frac{J_i}{J_s}\right)_{Q_{\alpha,}=0} = - \frac{2\sigma}{2-\sigma} \left(\frac{\delta P}{P}\right)_{Q_{\alpha,}=0} \quad . \quad (VII-3-3)$$

Thermodynamic Expression for $(J_i)_{Q_{\alpha,}=0}$

The thermodynamic Equation (I-5-1) for J_i may be rewritten in terms of U for $Q_{\alpha,} = 0$ as

$$(J_i)_{Q_{\alpha,}=0} = RL_{ii} \left[- \left(\frac{\delta P}{P}\right)_{Q_{\alpha,}=0} + U \left(\frac{\delta T_k}{2T}\right)_{Q_{\alpha,}=0} \right] \quad . \quad (VII-3-4)$$

This expression for $(J_i)_{Q_{\alpha,}=0}$ must be consistent with the kinetic expression given by Equation (VII-3-3); however, before equating them we shall determine $(\delta T_k)_{Q_{\alpha,}=0}$ from energy considerations.

Conservation of Energy

The conservation of energy applied to Figure 16 requires that

$$J_{u4} + J_{u3} - J_{u2} = J_{u1} \quad (\text{VII-3-5})$$

which for $Q_{\alpha,} = 0$ becomes

$$2 RT_{fi} (1 - \nabla) J_{i2} + 2 RT_{fi} \nabla J_s - 2 RT_{fi} J_{i2} = \frac{5}{2} RT_g (J_i)_{Q_{\alpha,}=0} - \left[(q/A)_g \right]_{Q_{\alpha,}=0} \cdot \quad (\text{VII-3-6})$$

This equation may be linearized to yield

$$\left[(q/A)_g \right]_{Q_{\alpha,}=0} = \frac{1}{2} RT (J_i)_{Q_{\alpha,}=0} \cdot \quad (\text{VII-3-7})$$

The heat transfer in the vapor $\left[(Q/A)_g \right]_{Q_{\alpha,}=0}$ is related to the transport coefficients K and L_k by Equation (I-5-7).

$$\left[(q/A)_g \right]_{Q_{\alpha,}=0} = \frac{K}{K+1} h_{fg} (J_i)_{Q_{\alpha,}=0} + \frac{L_k}{T^2} (\delta T_k)_{Q_{\alpha,}=0} \cdot \quad (\text{VII-3-8})$$

Eliminating $\left[(q/A)_g \right]_{Q_{\alpha,}=0}$ from Equations (VII-3-7) and (VII-3-8) results in the expression for $(\delta T_k)_{Q_{\alpha,}=0}$

$$(\delta T_k)_{Q_{\alpha,}=0} = \frac{1}{2L_k} RT^3 (J_i)_{Q_{\alpha,}=0} (1 - U) \cdot \quad (\text{VII-3-9})$$

Thus for the perturbation $Q_{\alpha,}$ to vanish, (δT_k) must be related to J_i by Equation (VII-3-9). This relationship is in terms of experimentally determined quantities.

Calculation of L_{ii}

Substitution of $(\delta T_k)_{Q_{\alpha,}=0}$ from Equation (VII-3-9) into Equation (VII-3-4) yields

$$(J_i)_{Q_{\alpha},=0} = - \left[\frac{1}{RL_{ii}} - \frac{RU(1-U)}{4L_k} \right]^{-1} \left(\frac{S P}{P} \right)_{Q_{\alpha},=0} \quad (\text{VII-3-10})$$

The coefficient RL_{ii} is obtained by substituting Equation (I-5-5) for L_k with $\gamma = 1.667$ (monatomic gas) and by equating the expressions for J_i given by Equations (VII-3-3) and (VII-3-10). The result is

$$RL_{ii} = J_s C_v \left[\frac{1}{C_v U(1-U)} \right] \left[1 + \frac{1}{16} \right], \quad (\text{VII-3-11})$$

where

$$C_v = \frac{2\gamma}{2-\gamma} \quad (\text{VII-3-12})$$

Since the experimental value of U is approximately 0.25 and since $0 \leq \gamma \leq 1$, Equation (VII-3-11) may be rewritten with sufficient accuracy as

$$RL_{ii} \approx \frac{2\gamma}{2-\gamma} J_s, \quad (\text{VII-3-13})$$

which is the same relationship obtained previously in Section I-5 from Schrage's theory.

General Expression for J_i

The general expression for J_i is given by the thermodynamic Equation (I-5-1) with RL_{ii} given by (VII-3-11)

$$J_i = J_s C_v \left[\frac{1}{C_v U(1-U)} \right] \left[- \frac{S P}{P} + U \frac{S T_k}{2T} \right] \quad (\text{VII-3-14})$$

Discussion of Analysis

It should be pointed out that we do not attempt to calculate the general equation for J_i from kinetic theory; instead we use the thermodynamic equation for J_i . The reason for this is that in the general case when $Q_{\alpha_i} \neq 0$, we do not know the exact distribution at α' . The kinetic theory model is used to obtain a relation for L_{ii} (Equation (VII-3-11)). This is obtained by considering the special case $Q_{\alpha_i} = 0$. We do not predict a value for U as this would require a knowledge of the exact distribution at α' . Instead we let U take on values consistent with experiment.

It is important to note that the coefficient σ appearing in Schrage's equation (I-3-5) is, for all practical purposes, the same as that found in the present analysis (Equation (VII-3-11)); therefore, even though Schrage's model does not yield the correct value of U , it does result in an equation which, in conjunction with experimental results, yields sufficiently accurate values of the condensation or evaporation coefficient.

Alternative Description

In the preceding analysis we have taken δT to be the difference between the temperature defined by the intercept of the vapor temperature profile with the liquid surface and the temperature T_{fi} as shown in Figure 16. This is the same as the temperature difference δT_k used by Kennard. This choice is, however, arbitrary. We could just as well, for example, have chosen the difference between T_{fi} and the intercept at a distance λ from the interface. Though the choice of δT is arbitrary, it is important to be consistent throughout the analysis. When the definition of δT is changed so also do the expressions for L_k and K (or U).

It is of advantage to define δT to be equal to δT_c such that when $Q_{\alpha, i} = 0$, δT_c is also equal to zero. With this definition the $Q_{\alpha, i} = 0$ experiment is also the isothermal experiment, and as is shown in Appendix C, the general equation for J_i becomes

$$J_i = J_s \frac{2\sigma}{2 - \sigma} \left[-\frac{\delta P}{P} + \frac{\delta T_c}{2T} \right] \quad (\text{VII-3-15})$$

This equation is identical with the linearized form of Schrage's equation (I-3-5) except that the definition, and therefore the value of the δT term, is different. The quantity δT_c as shown in Appendix C is given by

$$T_c = T_c - T_{fi} \quad (\text{VII-3-16})$$

where T_c is the value of the intercept of the vapor temperature profile extrapolated into the liquid a distance $c\lambda$ from the interface (λ is the mean free path in the vapor). The quantity c is related to U by the following expression which is derived in Appendix C.

$$c = \frac{1 - U}{2} \quad (\text{VII-3-17})$$

Using the experimental value of $U = 0.27$, we see that $c = 0.365$.

VIII. CONCLUSIONS

In the present investigation it was found that the evaporation or condensation coefficient ∇ , measured during the steady-state evaporation experiment, is higher than that obtained previously in condensation experiments. It was also found that contamination of the liquid surface results in low values of ∇ . Similarly, contamination in the form of non-condensable gases during previous condensation tests resulted in low values of ∇ . This suggests that the contamination in the evaporation experiment was maintained at a lower level than that attained during the condensation tests.

The results also suggest that ∇ measured during evaporation may not decrease with increasing interface temperatures as it does for the condensation data.

From the measured values of the transport coefficient K (or U) and the analysis presented in Section VII-2, we conclude that the events taking place at the liquid-vapor interface during the phase change cannot be represented completely by half maxwellian velocity distributions.

From the results of the analysis presented in Section VII-3 where we allowed for non-maxwellian velocity distributions, we conclude that even though Schrage's equation is not exact, it is a good approximation to use this equation in conjunction with experimental measurements to arrive at the condensation coefficient ∇ .

IX. RECOMMENDATIONS

The results of the steady-state evaporation experiment suggest that the coefficient \bar{V} may not decrease with increasing values of interface temperature as is found in the condensation data. It is thus recommended that the existing steady-state evaporation experimental apparatus be modified so that data can be taken at higher values of interface temperature.

The range over which the rates of phase change were varied in the present study did not show any non-linear effects. It would be of interest to carry out an experimental program to determine when the non-linear effects, which are excluded in the linear irreversible thermodynamic analysis, become important.

An attempt should be made to theoretically predict the transport coefficient U from an analysis employing the Boltzmann equation. This would replace the present method of describing the kinetics which employs an equilibrium distribution plus a correction term Q (Section VII-3).

BIBLIOGRAPHY

1. Nusselt, W., *Zeitsch. d. ver. deutsch. Ing.*, 60, 541, (1916).
2. Kroger, D. G., "Heat Transfer During Film Condensation of Potassium Vapor," Sc.D. Thesis, M.I.T., Sept., 1966.
3. Sukhatme, S. and Rohsenow, W., "Heat Transfer During Film Condensation of a Liquid Metal Vapor," Report No. 9167-27, Dept. of Mech. Eng'g., M.I.T., April, 1964.
4. Schrage, R. W., A Theoretical Study of Interphase Mass Transfer, Columbia University Press, New York, (1953).
5. Bornhorst, W. J., "Irreversible Thermodynamics of a Phase Change," Ph.D. Thesis, M.I.T., June, 1966.
6. Hatsopoulos, G. N. and Keenan, J. H., Principles of General Thermodynamics, John Wiley and Sons, Inc., New York, 1965.
7. Kennard, E. H., Kinetic Theory of Gases, McGraw-Hill Book Co., Inc., New York, 1938.
8. Wachman, H. Y., "The Thermal Accommodation Coefficient: A Critical Survey," *ARS*, Vol. 32, No. 9, Jan. 1962.
9. Misra's data are presented by:

Wilhelm, D. J., "Condensation of Metal Vapors: Mercury and the Kinetic Theory of Condensation," ANL-6948, 1964.
10. Subbotin, V. I., Ivanovsky, M. N., Sorokin, V. P., Chulkov, V. A., *Teplofizika Vysokih Temperatur*, No. 4, (1964).
11. Barry, R. E., Ph.D. Thesis, University of Michigan, (1965).
12. Aladyev, I. T., et al., "Thermal Resistance of Phase Transition with Condensation of Potassium Vapor," Proceedings of the Third International Heat Transfer Conference, (1966).
13. Labuntsov, P. A. and Smirnov, S. I., "Heat Transfer in Condensation of Liquid Metal Vapors," Proceedings of the Third International Heat Transfer Conference, (1966).
14. Jeans, J., An Introduction to the Kinetic Theory of Gases, Cambridge Press, (1962).
15. Ditchburn, R. W. and Gilmour, J. C., "The Vapor Pressures of Monatomic Vapors," *Rev. Mod. Phys.*, Vol. 13, Oct. 1941.

16. Teagan, W. P., "Heat Transfer and Density Distribution Measurements Between Parallel Plates in the Transition Regime," Doctoral Thesis, M.I.T., June, 1967.
17. Weatherford, W. D., Jr., Tyler, J. C., and Ku, P. M., "Properties of Inorganic Energy-Conversion and Heat-Transfer Fluids for Space Applications," WADD Technical Report 61-96, Nov., 1961.
18. The International Nickel Co., Inc., Technical Bulletin T-15.
19. Kline, S. J. and McClintock, F. A., "Describing Uncertainties in Single-Sample Experiments," Mechanical Engineering, Vol. 75, January, 1953.
20. Knudsen, M., The Kinetic Theory of Gases, Methuen and Co. and John Wiley and Sons, Inc., New York, 1950.
21. Volmer and Esterman's results are discussed in Reference 20.

APPENDIX A - DERIVATION OF J_i EQUATION FROM KINETIC THEORY

In this Appendix the kinetic expression for J_i is derived. The reason for doing this is to show that the condensation coefficient as it appears in Equation (I-3-1) must depend only on the temperature of the liquid T_{fi} (or equivalently P_s).

Consider a control surface α' at the liquid surface illustrated in Figure 16. It is assumed that the velocity distribution of molecules crossing α' to the left is a half maxwellian at the temperature P_2 and temperature T_2 . It is assumed that the molecules crossing α' to the right are composed of two parts the first of which is those molecules emitted from the liquid. This emission process is assumed to depend only on the temperature of the liquid surface, and the rate of emission for nonequilibrium conditions is obtained by considering an equilibrium situation. The second part of those crossing α' to the right is composed of incident molecules which have been reflected from the surface.

The maxwellian velocity distribution at the temperature T_2 and pressure P_2 is given by

$$f_2 = \frac{P_2}{mRT_2(2 RT_2)^{3/2}} e^{-\frac{1}{2 RT_2}(u^2 + v^2 + w^2)} \quad (A-1)$$

By a half maxwellian distribution, it is meant that the limits on the velocity u are $-\infty \leq u \leq 0$ for the incident distribution and $0 \leq u \leq \infty$ for the emitted distribution while v and w are allowed to vary from $+\infty$ to $-\infty$. The velocity u is in a direction perpendicular to the interface. The velocities v and w are perpendicular to each other and, to u .

The net rate of evaporation as given by

$$J_i = J_{i3} + J_{i4} - J_{i2} \quad (A-2)$$

Integration of the half-maxwellian distribution function f_2 yields

$$J_{i2} = \frac{P}{\sqrt{2\pi RT_2}} \quad (A-3)$$

The flux J_{i4} is related to J_{i2} by the condensation coefficient ∇ which is defined in the usual way as the fraction of J_{i2} which condenses.

$$J_{i4} = \left[1 - \nabla(T_{fi}, P_g, T_g) \right] J_{i2} \quad (A-4)$$

In Equation (A-4) we allow ∇ to be a function of the temperature and pressure of both the liquid and vapor.

To obtain an expression for J_{i3} , we consider an equilibrium situation where

$$P_2 = P_s \quad (A-5)$$

$$T_2 = T_{fi} \quad (A-6)$$

For such a situation the evaporation rate $J_i = 0$ thus

$$J_{i2}^E - J_{i3}^E - J_{i4}^E = 0 \quad (A-7)$$

where

$$J_{i2}^E = \frac{P_s}{\sqrt{2\pi RT_{fi}}} \quad (A-8)$$

and

$$J_{i4}^E = \left[1 - \nabla^E(T_{fi}, P_g = P_s, T_g = T_{fi}) \right] J_{i2}^E \quad (A-9)$$

The superscript E denotes equilibrium conditions. Combining Equations (A-7) thru (A-9) yields

$$J_{i3}^E = J_{i2}^E \nabla^E(T_{fi}) = \frac{P_s}{\sqrt{2\pi RT_{fi}}} \nabla^E(T_{fi}) \quad (A-10)$$

where

$$\nabla^E(T_{fi}) = \nabla^E(T_{fi}, P_g = P_s, T_g = T_{fi}) \quad (A-11)$$

is the value of ∇ at equilibrium conditions.

In general properties of a liquid are weak functions of pressure, for example, the vapor pressure (Poynting effect), surface tension, and so on. It is thus not unreasonable to suspect that J_{i3} is at the most a weak function of the pressure. If we assume that J_{i3} is independent of the pressure, then

$$J_{i3}(T_{fi}, P_g) = J_{i3}^E(T_{fi}, P_s) \quad (A-12)$$

For the nonequilibrium situation, the rate of phase change

$$J_i = J_{i3} + J_{i4} - J_{i2} \quad (A-13)$$

thus becomes

$$J_i = \frac{P_s \nabla^E}{\sqrt{2\pi RT_{fi}}} - \frac{P_2 \nabla(T_{fi}, P_g, T_g)}{\sqrt{2\pi RT_2}} \quad (A-14)$$

Equation (A-14) is similar to that given by Schrage for the rate of phase change differing in the term $P_2 / \sqrt{2\pi RT_2}$, the difference arising from the assumed distribution for f_2 . He assumes a half maxwellian, characterized by the parameters $T_2 = T_g$ and $P_2 = P_g$. He also includes a superimposed bulk flow velocity in the distribution. In making his assumptions, one arrives at

$$J_{i1} = \frac{P_s \sigma^E}{\sqrt{2\pi RT_{fi}}} - \frac{\Gamma P_{gi} \sigma(T_{fi}, P_g, T_g)}{\sqrt{2\pi RT_{gi}}} \quad (A-15)$$

where Γ arises from the bulk flow velocity in the incident distribution.

To arrive at the generally used Equation (I-3-1) for the mass flux J_i , the additional assumption that

$$\sigma(T_{fi}, P_g, T_g) = \sigma^E(T_{fi}) \quad (A-16)$$

must be made. What this assumption requires is that the condensation coefficient be dependent only on the liquid temperature T_{fi} .

APPENDIX B - CONSIDERATION OF EXPERIMENTAL ERRORS

B-1. Uncertainty Intervals

In order to estimate the reliability of the results obtained, the method of presenting the uncertainties incurred in the experiment as suggested by Kline and McClintock⁽¹⁶⁾ is used. The uncertainty interval ω_X for a quantity $X(\nu_i)$ is computed from

$$\omega_X = \sqrt{\sum \nu_i \left(\frac{\partial X}{\partial \nu_i} \omega_{\nu_i} \right)^2} \quad (B-1)$$

where the sum is over the quantities ν_i upon which the result X depends, and ω_{ν_i} is the estimated error in the quantity ν_i . The values of ω_{ν_i} used are left up to the rational judgment of the observer. The results thus obtained indicate the credibility of this judgment.

B-2. Major Errors in U

In computing U it is found that the major sources of error are caused by errors in the vapor temperature T_g and the liquid interface temperature T_{fi} . The major sources of error in T_{fi} are those due to T_{NI} and h_{Hg} . Concerning ourselves with only these major errors, we obtain

$$\omega_U = U \sqrt{\left(\frac{\omega_{T_g}}{\delta T} \right)^2 + \left(\frac{\omega_{T_{NI}}}{\delta T} \right)^2 + \left(\frac{(\Delta T / \Delta X)_{Hg}}{\delta T} \omega_{h_{Hg}} \right)^2} \quad (B-2)$$

In terms of the symbols used in Table I, Equation (B-2) is rewritten as

$$TPEU \equiv \omega_U / U \quad (B-3)$$

$$= \sqrt{(PEUTG)^2 + (PEUTN)^2 + (PEUHG)^2} \quad (B-4)$$

The error in the vapor temperature $\omega_{T_{gi}}$ is estimated from the differences in the temperatures measured by the thermocouples in the vapor and is found to be the same as the accuracy found during the calibrations of the thermocouples which is $\pm 0.2^\circ\text{F}$.

The error in T_{NI} is estimated to be the difference in the values of T_{NI} computed from the four- and five-point least squares, straight lines drawn through the temperatures measured in the nickel. This error is also the same as that found in the thermocouple calibration.

Because of reproducibility the error in the liquid depth is taken to be 0.0015 inch for all the data.

B-3. Major Errors in ∇

In estimating the errors in ∇ , it is sufficient to use the approximate expression for ∇

$$\frac{2\nabla}{2-\nabla} = (J_i)_{ss} \frac{\sqrt{2\pi RT}}{(\delta P)_{ss}} \quad (\text{B-5})$$

as the term $(\frac{\delta T}{2T})_{ss}$ is experimentally found to be small compared to $(\delta P/P)_{ss}$ in Equation (V-1-4).

Considering only the major contributions to the error in ∇ , which are errors due to P_g , T_{NI} , and h_{Hg} , we obtain for the error interval of ∇ the following:

$$\omega_{\nabla} = \nabla \left(\frac{2-\nabla}{2} \right) \sqrt{ \left(\frac{\omega_{P_g}}{P} \right)^2 + \left(\frac{\partial P_s}{\partial T_{fi}} \frac{\omega_{T_{NI}}}{\delta P} \right)^2 + \left(\frac{\partial P_s}{\partial T_{fi}} \left(\frac{\Delta T}{\Delta X} \right)_{H_g} \frac{\omega_{h_{Hg}}}{\delta P} \right)^2 } \quad (\text{B-6})$$

where $\partial P_s / \partial T_{fi}$ is the slope of the saturation pressure-temperature curve of mercury. In terms of the symbols used in Table I, Equation (B-6) becomes

$$\text{TPE} \nabla \equiv \frac{\omega_0}{\nabla} \quad (\text{B-7})$$

$$= \sqrt{(\text{PE} \nabla \text{HG})^2 + (\text{PE} \nabla \text{TNI})^2 + (\text{PE} \nabla \text{HHG})^2} \quad (\text{B-8})$$

The error in the system pressure P_g is taken to be 0.02 inch of water. This accounts for the error in reading the manometer, the smallest division of which is 0.01 inch of water. An exception to this is for data point 15, 16, 17, and A where a manometer having a smallest division of 0.05 inch of water was used. The above considered errors are tabulated in Table I.

B-4. Additional Errors

In the above considerations it was assumed that no error was involved in assuming that the rate of evaporation was given by the slope of the temperature gradient in the nickel and the pertinent physical properties of the materials. The errors introduced by incorrect values of material properties are expected to be small compared to the errors in measured quantities. For example, the saturation pressure-temperature data used are accurate to 2 percent.⁽¹⁵⁾ A calibration was performed to check out the validity of the relationship between the rate of evaporation and the nickel-block temperature gradient given by Equation (V-6). The net rate of evaporation was determined by measuring with scales the supply flow rate and overflow rate of liquid mercury and taking the difference.

The net rate of evaporation measured was found to be 6 percent larger than that calculated from the temperature gradient and the area of the leg of the nickel block. This result was expected as the area of the liquid-vapor interface is larger than the area of the leg of the nickel block, and end effects should cause the above result. This calibration is only a check and does not yield a specific value of any error incurred in assuming Equation (V-6). Because of the calibration, however, it can be said with confidence that any such error is small compared to the major errors considered previously.

Another possible source of error is that due to a non-linear temperature profile in the liquid. Tests were run at different combinations of liquid depth and temperature gradients resulting in a wide range of Grashoff numbers. No systematic error was detected.

Thermal contact resistance at the liquid mercury-solid nickel interface would also introduce an error. For a clean wetted surface, however, this resistance should be negligible. In addition, if such an error exists, the true value of the liquid interface temperature T_{fi} and, therefore, $P_s(T_{fi})$ would be lower than that used in the present calculation. This would result in lower values of both δT and δP thereby yielding smaller values for U and larger values of \bar{V} .

During testing it was not possible to maintain a perfect, steady state condition. To detect any errors due to non-steady state, tests were run with measured quantities increasing with time and decreasing with time and at different rates of change. No such errors were detected.

The error in the manometer reference pressure is estimated from the reading of a vacuum thermocouple gage to be 0.01 inch of water, and this error is included in the upper bound on \bar{V} in Figure 13.

If the walls bounding the vapor are at a temperature different from that of the vapor, there could be an error in the vapor temperature measurement due to radiant heat transfer between the walls and the thermocouples in the vapor. In addition, there would be heat transfer to the vapor which should be zero for steady-state evaporation. A radiation shield consisting of two concentric cylinders was placed around the vertical thermocouples. A thermocouple was also placed in the wall. A test was run with the wall temperature, the temperature of the horizontal probe, and the temperature of the vertical probes all at the same value. The results of this test were in accord with those obtained without the shield thereby verifying that radiation errors were not present.

The reproducibility of the results was affirmed by disassembly and cleaning of the apparatus. This was done by necessity when the surface accidentally became dry. When this happened it was necessary to disassemble the apparatus and reclean the nickel surface with hydrochloric acid.

APPENDIX C - DEVELOPMENT OF THE ALTERNATIVE DESCRIPTION (SECTION VII-3)

It was pointed out in Section VII-3 that there is freedom of choice in the definition of δT . The δT_k chosen in Section VII is the same as that used by Kennard.⁽⁷⁾ In this Appendix we shall choose δT to be equal to δT_c where δT_c is such that when $Q_{\alpha} = 0$ (Section VII-3) δT_c is also equal to zero.

With this choice of $\delta T = \delta T_c$, we proceed to obtain the general equation for J_i in terms of δT_c . This relationship is found by transforming Equation (VII-3-14) which is reproduced here.

$$J_i = J_s C_{\sigma} \left[\frac{1}{C_{\sigma} U (1 - U)} \right] \left[- \frac{\delta P}{P} + U \frac{\delta T_k}{2T} \right]. \quad (C-1)$$

The transformation is accomplished by relating δT_c to δT_k . Referring to Figure 17 we obtain the following relationship:

$$\delta T_c = \delta T_k - \frac{(q/A)_g}{k_g} c \lambda \quad (C-2)$$

where λ is the mean free path in the gas, and $c \lambda$ locates the distance from the interface where the extrapolated vapor temperature equals T_c . From the thermodynamic Equation (I-5-2), the energy flux is given by

$$J_u = \left(h_g - \frac{K}{K+1} h_{fg} \right) J_i - \frac{L_k}{T} T_k \quad (C-3)$$

The energy flux at α'' (Figure 16) is also given by the usual bulk flow relation

$$J_u = h_g J_i - (q/A)_{\alpha''} \quad . \quad (C-4)$$

Equations (C-3) and (C-4) may be combined to yield the following for

$$(q/A)_{\alpha''}$$

$$(q/A)_{\alpha''} = \frac{K}{K+1} h_{fg} J_i + L_k \frac{\delta T_k}{T^2} \quad . \quad (C-5)$$

Substitution of $(q/A)_{\alpha''}$ from Equation (C-5) into (C-2) and using Equation (V-1) to relate K to U results in the following expenses for δT_k

$$\delta T_k = \frac{T_c + \frac{c \lambda}{k_g} U \frac{RT}{2} J_i}{1 - c \left(\frac{L_k/T^2}{k_g/\lambda} \right)} \quad . \quad (C-6)$$

The ratio $(L_k/T^2)/(k_g/\lambda)$ is found to be a constant

$$(L_k/T^2)/(k_g/\lambda) = 2 \quad . \quad (C-7)$$

This result evolves when L_k is given by Equation (I-5-5) with $\alpha = 1$ and $\gamma = 1.667$ (monatomic gas) and when the conductivity of the vapor phase k_g is given by the kinetic expression for thermal conductivity.⁽¹⁴⁾

$$k_g = \frac{1}{2} \rho \bar{v} \lambda C_v, \quad (C-8)$$

where \bar{v} is the mean molecular speed, and C_v is the specific heat constant volume. For the maxwellian velocity distribution, \bar{v} is given by⁽¹⁴⁾

$$\bar{v} = \sqrt{\frac{8RT}{\pi}} \quad . \quad (C-9)$$

Substitution of Equations (C-6) and (C-7) into (C-1) yields

$$J_i = \theta J_s C_{\sigma} \left[-\frac{\delta P}{P} + \frac{U}{1-2c} \frac{\delta T_c}{2T} \right] \quad (C-10)$$

where

$$\theta = \frac{Z}{1 - Z U^2 \left(\frac{c}{1-2c} \right) \frac{\lambda R}{k} \frac{1}{4} J_s C_{\sigma}} \quad (C-11)$$

and

$$Z = \frac{1}{1 + \frac{U(1-U)}{16} C_{\sigma}} \quad (C-12)$$

The relationship between c and U is found as follows: We first find the relationship between L_k and L_c where L_c is defined as

$$L_c = \frac{(J_u)_{J_i=0} T^2}{(\delta T_c)_{J_i=0}} \quad (C-13)$$

The coefficient L_c is the equivalent of L_k when δT_c is chosen for δT . Since the energy flux

$$(J_u)_{J_i=0} = (q/A)_g \quad (C-14)$$

must be independent of the choice of definition of δT , we may write

$$L_c (\delta T_c)_{J_i=0} = L_k (\delta T_k)_{J_i=0} \quad (C-15)$$

From Equations (C-15), (C-14), (C-7), and (C-2), the following relationship between L_c and L_k is obtained

$$\frac{L_c}{L_k} = \frac{1}{1 - 2c} \quad . \quad (C-16)$$

The quantity U_c , which is the equivalent of U when δT_c is chosen for δT , is given by

$$U_c = - \frac{2 L_c}{RT^3} \left(\frac{\delta T_c}{J_i} \right)_{ss} \quad (C-17)$$

while the expression for U is given by

$$U = - \frac{2 L_k}{RT^3} \left(\frac{\delta T_k}{J_i} \right)_{ss} \quad (C-18)$$

By combining Equations (C-17), (C-18), and (C-16) and noting that

$$(\delta T_c)_{ss} = (\delta T_k)_{ss} \quad , \quad (C-19)$$

we obtain

$$\frac{U}{1 - 2c} = U_c \quad . \quad (C-20)$$

Finally we obtain the value of U_c . To do this we consider the $Q_{\alpha,} = 0$ situation which is also the $\delta T_c = 0$ case. The conservation of energy applied to Figure 16 for $Q_{\alpha,} = 0$ requires that

$$\left[(q/A)_g \right]_{\delta T_c=0} = \frac{1}{2} RT(J_i)_{\delta T_c=0} \quad . \quad (C-21)$$

The heat transfer in the vapor for $\delta T_c = 0$ is also given by Equation (1-5-7)

$$\left[(q/A)_g \right]_{\delta T_c=0} = \frac{K_c}{K_c + 1} h_{fg}(J_i)_{\delta T_c=0} \quad (C-22)$$

Combining Equations (C-21) and (C-22) yields

$$\frac{K_c}{K_c + 1} \frac{2h_{fg}}{RT} = 1 \quad (C-23)$$

This, however, is the definition of U_c ; thus

$$U_c = 1 \quad (C-24)$$

and from Equation (C-20), we obtain the desired relation between U and c

$$U = 1 - 2c \quad (C-25)$$

On substituting (C-25) into Equations (C-12), (C-11), and (C-10), we obtain the desired relation for J_i in terms of δT_c

$$J_i = J_s C_{\sigma} \left[-\frac{\delta P}{P} + \frac{\delta T_c}{2T} \right] \quad (C-26)$$

It should be pointed out that for the $\delta T_c = 0$ situation, Equation (C-26) reduces to the kinetic Equation (VII-3-9) for J_i as it must.

It is noteworthy that the heat of transport q^* , which for $\delta T_c = 0$ is given by $\left[(q/A)_g/J_i \right]_{\delta T_c=0}$, has the value $\frac{1}{2} RT$. This is the same as the heat of transport for a perfect gas flowing through a Knudsen plug. (6)

APPENDIX D

BIOGRAPHICAL NOTE

Date of Birth: June 21, 1940

Place of Birth: Brooklyn, New York

Education:

September 1958 University of Miami, Coral Gables, Florida
February 1962 S.B. Degree in Mechanical Engineering

September 1963 Massachusetts Institute of Technology
June 1965 Cambridge, Massachusetts
S.M. Degree in Mechanical Engineering
Field: Fluid Mechanics
Title: Research Assistant

September 1965 Massachusetts Institute of Technology
Present Cambridge, Massachusetts
Doctoral Student in Mechanical Engineering
Field: Thermodynamics; Heat Transfer
Title: Research Assistant

Professional Experience:

February 1962 to Employed as a Research Engineer by the Northern
September 1963; Research and Engineering Corporation in Cambridge,
Massachusetts. Concerned with high heat flux heat
June 1964 to transfer problems, the development of zero-gravity
September 1964; liquid-vapor separation techniques, centrifugal,
and axial turbomachinery blade-design research and
June 1965 to development.
September 1965

Papers:

Hiser, H. W. and Adt, R. R., Jr.
"Precipitation Echo Heights in South Florida,"
Ninth Weather Radar Conference, Kansas City,
Missouri, Oct. 23-26, 1961.

Blatt, T. A. and Adt, R. R., Jr.
"Boiling Heat Transfer and Pressure Drop
Characteristics of Freon 11 and Freon 13
Refrigerants," A.I.Ch.E., No. 132, 15th
National Meeting, Buffalo, N. Y.,
May 5-8, 1963.

Papers: (Continued)

Blatt, T. A. and Adt, R. R., Jr.,
"The Effects of Twisted Tape Swirl Generators
on the Heat Transfer Rate and Pressure Drop
of Boiling Freon 11 and Water," A.S.M.E. Paper
No. 63-WA-42, Winter Annual Meeting, Philadelphia,
Pa., Nov. 17-22, 1963.

Honors and
Honorary and
Professional
Societies:

Graduated Magna Cum Laude and first in the
Engineering School of the University of
Miami.

Member of the University of Miami
Engineering Honor Society.

Member of Pi Mu Epsilon, Math Honor Society.

Member of Phi Kappa Phi, National Honor
Society.

Member of Sigma Xi, Scientific Research
Society.

Member of American Society of Mechanical
Engineers.

TABLE I - EXPERIMENTAL RESULTS

Test No.	Date	P_s atm	$-\delta P/P$	$-\delta T/T$	J_i	$\frac{\text{lbm}}{\text{hrft}^2}$	h_{Hg} in.	σ	U
1	12-5-66	0.0100	0.0313	0.00173	113	0.028	0.91	0.26	
2	12-7-66	0.0079	0.0655	0.00296	143	0.011	0.78	0.29	
3	12-16-66	0.0114	0.0282	0.00112	154	0.021	1.06	0.14	
4	12-21-66	0.00587	0.0452	0.00236	101	0.019	0.94	0.24	
5	1-9-67	0.0109	0.0688	0.00422	208	0.006	0.79	0.38	
6	1-9-67	0.0111	0.0675	0.00387	209	0.011	0.80	0.36	
7	1-9-67	0.0112	0.0606	0.00345	206	0.010	0.84	0.32	
8	1-9-67	0.0112	0.0492	0.00254	205	0.018	0.93	0.24	
9	1-9-67	0.0113	0.0463	0.00234	206	0.018	0.96	0.22	
10	1-9-67	0.0115	0.0395	0.00220	205	0.031	1.04	0.21	
11	1-12-67	0.0107	0.0624	0.00334	205	0.009	0.84	0.31	
12	1-12-67	0.0107	0.0624	0.00378	206	0.007	0.81	0.34	
13	1-12-67	0.0126	0.0360	0.00194	202	0.014	1.03	0.21	
14	1-12-67	0.0125	0.0417	0.00202	202	0.015	0.96	0.21	
15	1-17-67	0.0176	0.0209	0.00166	181	0.023	1.09	0.28	
16	1-17-67	0.0180	0.0251	0.00187	181	0.022	0.98	0.32	
17	1-17-67	0.0172	0.0254	0.00176	183	0.026	1.01	0.28	
18	1-19-67	0.0105	0.0511	0.00270	196	0.023	0.92	0.25	
19	1-19-67	0.0128	0.0404	0.00237	194	0.024	0.94	0.27	
20	1-19-67	0.0146	0.0370	0.00184	198	0.026	0.95	0.22	
21	1-19-67	0.0142	0.0373	0.00182	196	0.026	0.94	0.23	
22	1-19-67	0.0138	0.0337	0.00177	145	0.027	0.85	0.29	
23	1-19-67	0.0135	0.0397	0.00199	144	0.026	0.78	0.32	
24	1-19-67	0.0136	0.0417	0.00210	140	0.025	0.74	0.35	
25	1-19-67	0.0137	0.0370	0.00178	141	0.023	0.80	0.30	
26	1-19-67	0.0138	0.0403	0.00162	146	0.016	0.77	0.26	
27	1-19-67	0.0136	0.0297	0.00106	144	0.017	0.91	0.17	
28	5-5-67	0.0102	0.0472	0.00177	125	0.014	0.75	0.25	
A	12-14-67	0.0271	0.0481	0.00102	219	0.007	0.57	0.21	
B	12-21-66	0.0071	0.120	0.00696	152	0.014	0.59	0.57	
C	1-9-67	0.0101	0.151	0.00958	102	0.012	0.27	1.64	
D	1-9-67	0.0098	0.102	0.00621	105	0.015	0.40	1.00	
E	5-4-67	0.0259	0.535	0.0277	176	0.018	0.06	6.8	
F	5-6-67	0.0103	0.0673	0.00348	117	0.025	0.57	0.53	
G	5-6-67	0.0103	0.0612	0.00302	125	0.025	0.63	0.43	

* Symbols (see Appendix B)

- PEUTG = Percentage error in U due to error in measuring T
- PEUTN = Percentage error in U due to error in measuring T_{NI}^g
- PEUHHG = Percentage error in U due to error in measuring h_{Hg}
- PE σ PG = Percentage error in σ due to error in measuring P_{Hg}^g
- PE σ TN = Percentage error in σ due to error in measuring T_{NI}^g
- PE σ HHG = Percentage error in σ due to error in measuring h_{Hg}
- TPEU = Total percentage error in U
- TPE σ = Total percentage error in σ

The errors are plus or minus.

TABLE I - EXPERIMENTAL RESULTS
(Continued)

Test No.	PEUTG*	PEUTN	PEUHHG	TPEU	PEOPG	PEOTN	PEOHHG	TPEO
1								
2	9	3	16	19	6	2	7	9
3	22	17	44	52	7	5	13	16
4	11	8	15	18	10	4	7	12
5	6	5	16	18	4	3	10	11
6	6	5	18	19	4	3	10	11
7	7	6	19	21	4	3	10	12
8	10	11	26	30	5	5	12	13
9	5	11	28	31	5	5	12	14
10	17	13	30	37	5	6	13	15
11	7	5	20	22	4	2	10	11
12	13	4	18	22	4	2	10	11
13	13	11	33	37	5	4	14	16
14	24	7	32	41	5	3	13	14
15	14	11	34	38	18	6	19	27
16	13	13	30	35	17	8	18	25
17	7	14	32	36	17	8	18	25
18	5	15	24	28	5	7	11	14
19	5	10	26	29	5	5	13	15
20	7	15	34	38	5	6	14	16
21	7	18	34	39	5	7	14	16
22	27	8	26	39	6	4	13	14
23	6	9	23	25	5	4	11	13
24	12	7	21	25	6	4	11	13
25	14	9	25	30	6	4	11	14
26	15	3	29	33	5	1	11	13
27	35	3	43	55	6	1	13	15
28	0	4	23	23	6	1	9	11
A	6	19	63	90	6	4	14	17
B	4	1	7	8	4	8	5	7
C	4	4	4	7	3	3	3	5
D	6	2	6	9	4	2	5	6
E								
F	12	7	11	18	5	4	6	9
G	10	1	13	17	5	1	8	9

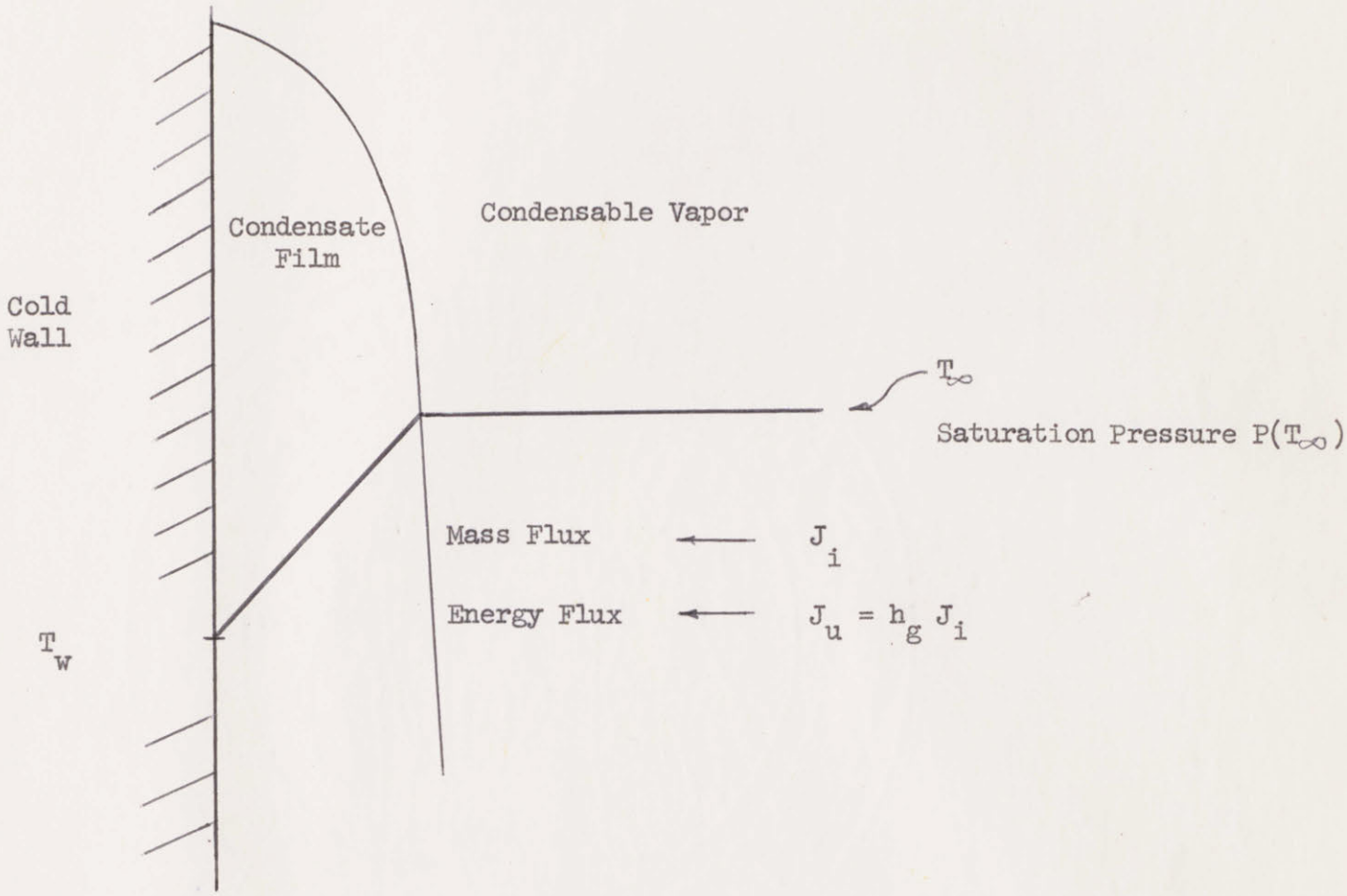


Figure 1 - Nusselt Model of Condensation

liquid

vapor

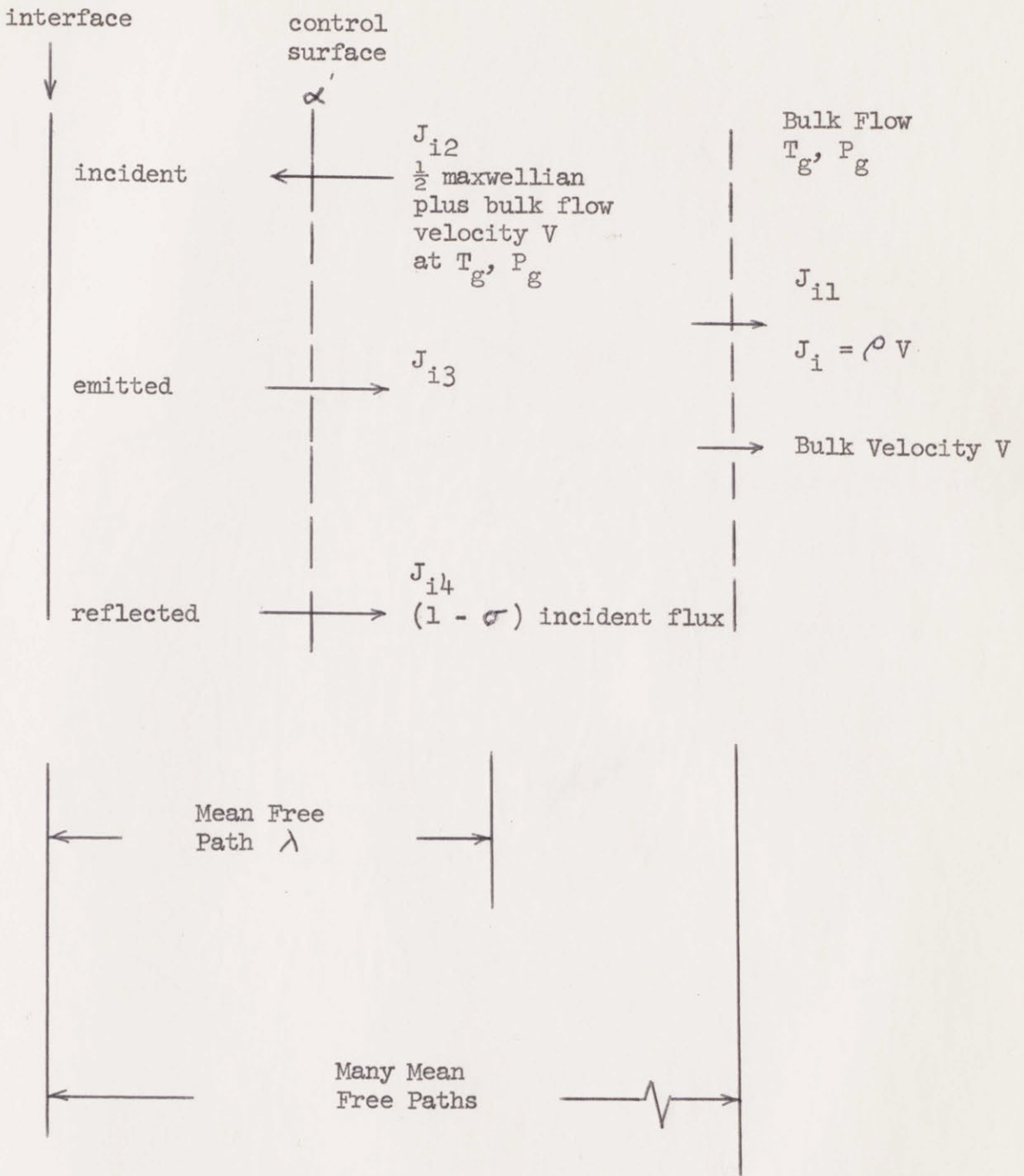


Figure 2 - Schrage's Kinetic Model of the Phase Change

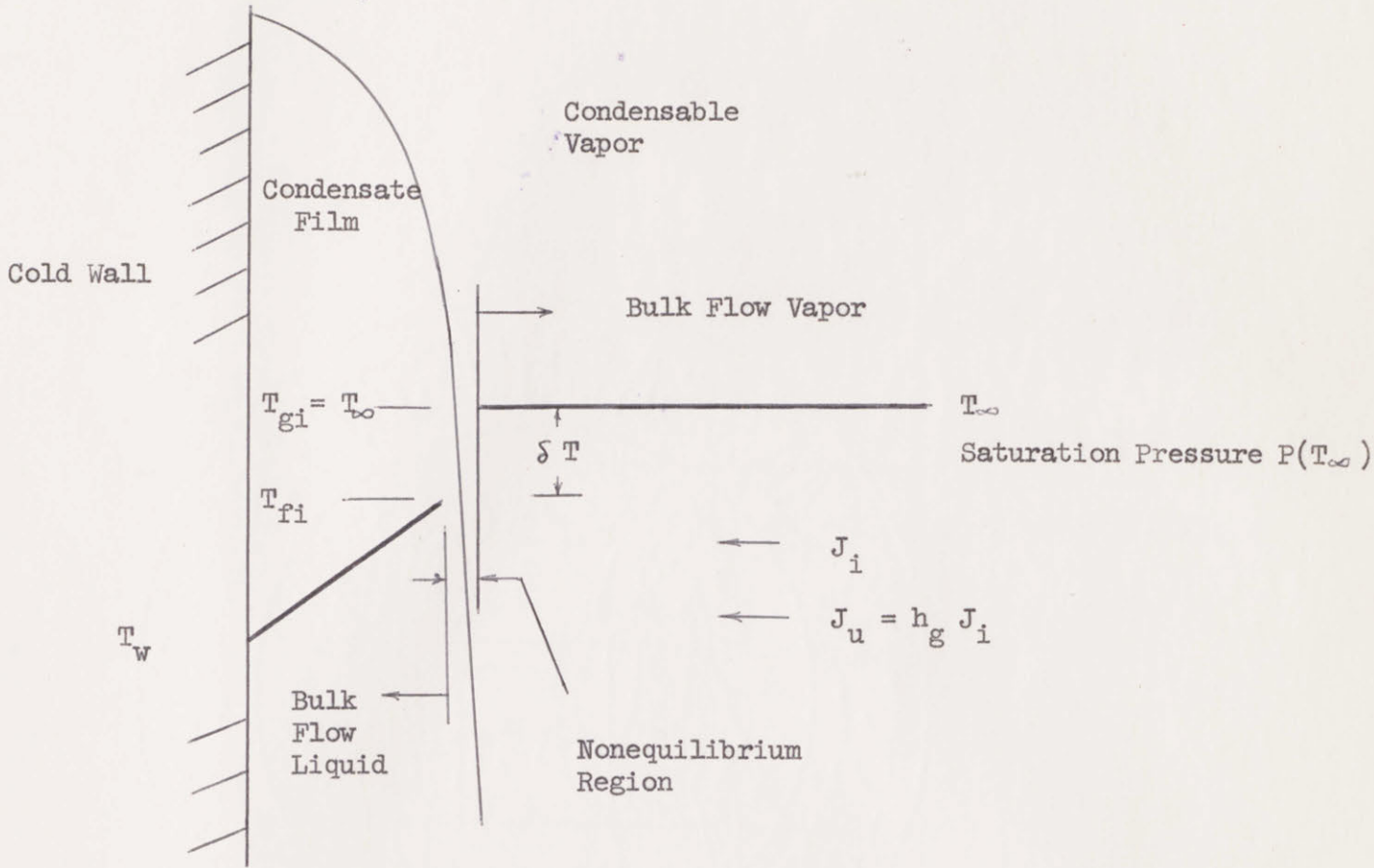


Figure 3 - Use of Schrage's Kinetic Analysis in the Condensation Problem

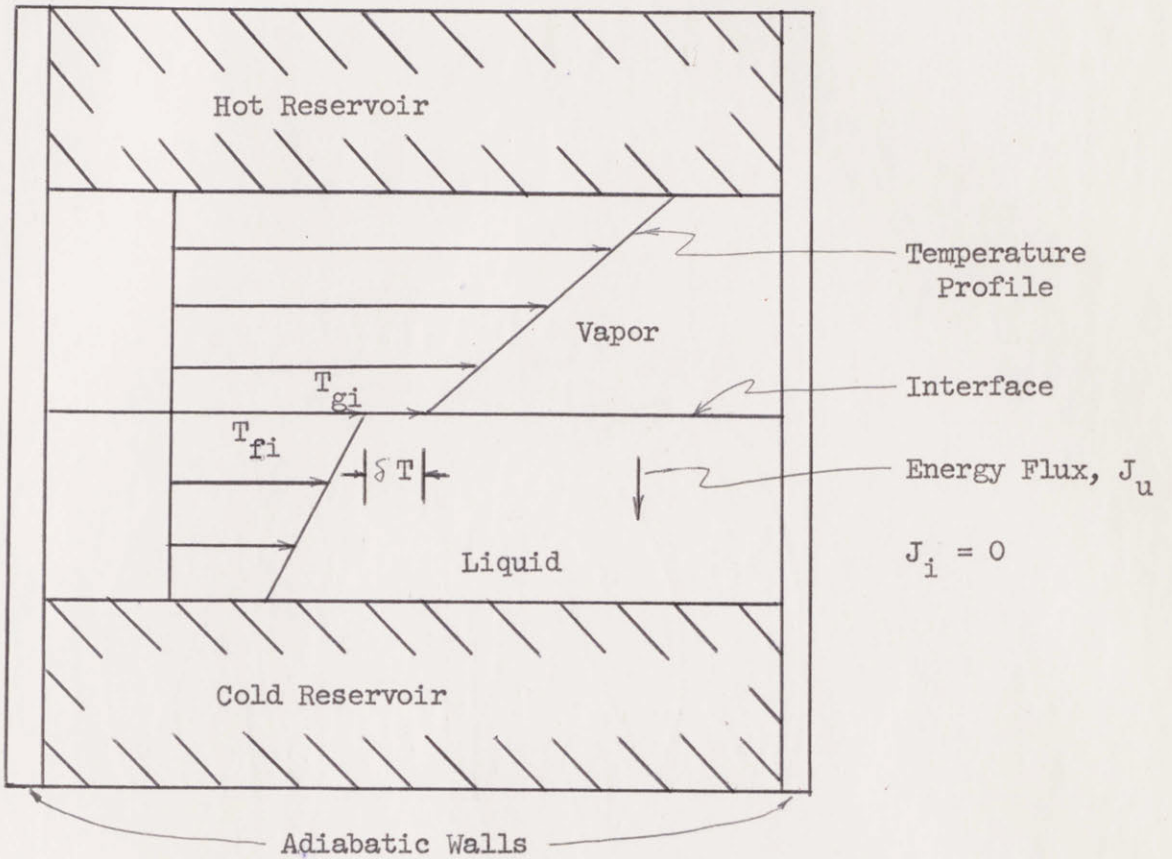


Figure 4 - No-Flow Experiment

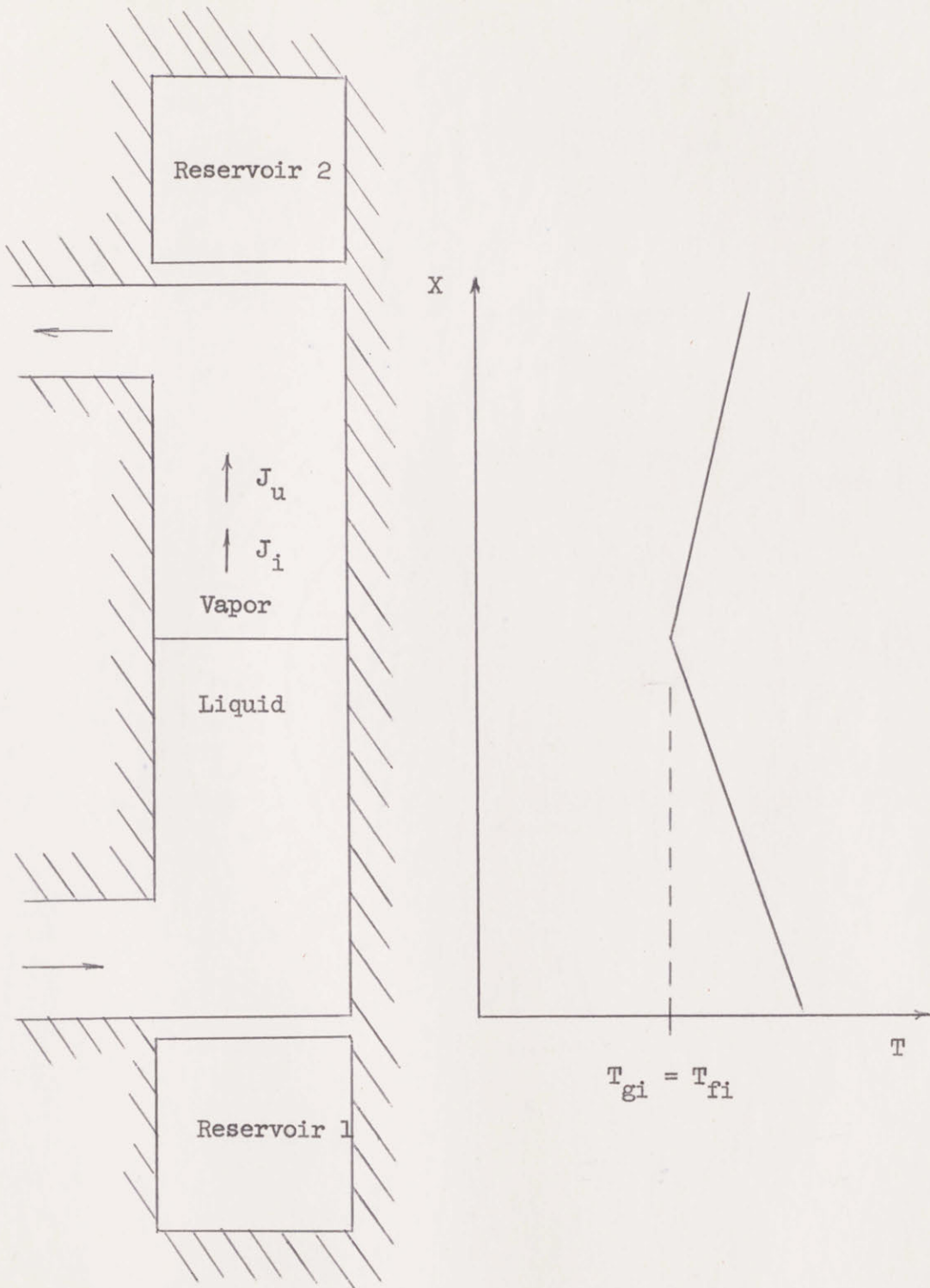


Figure 5 - Isothermal Experiment

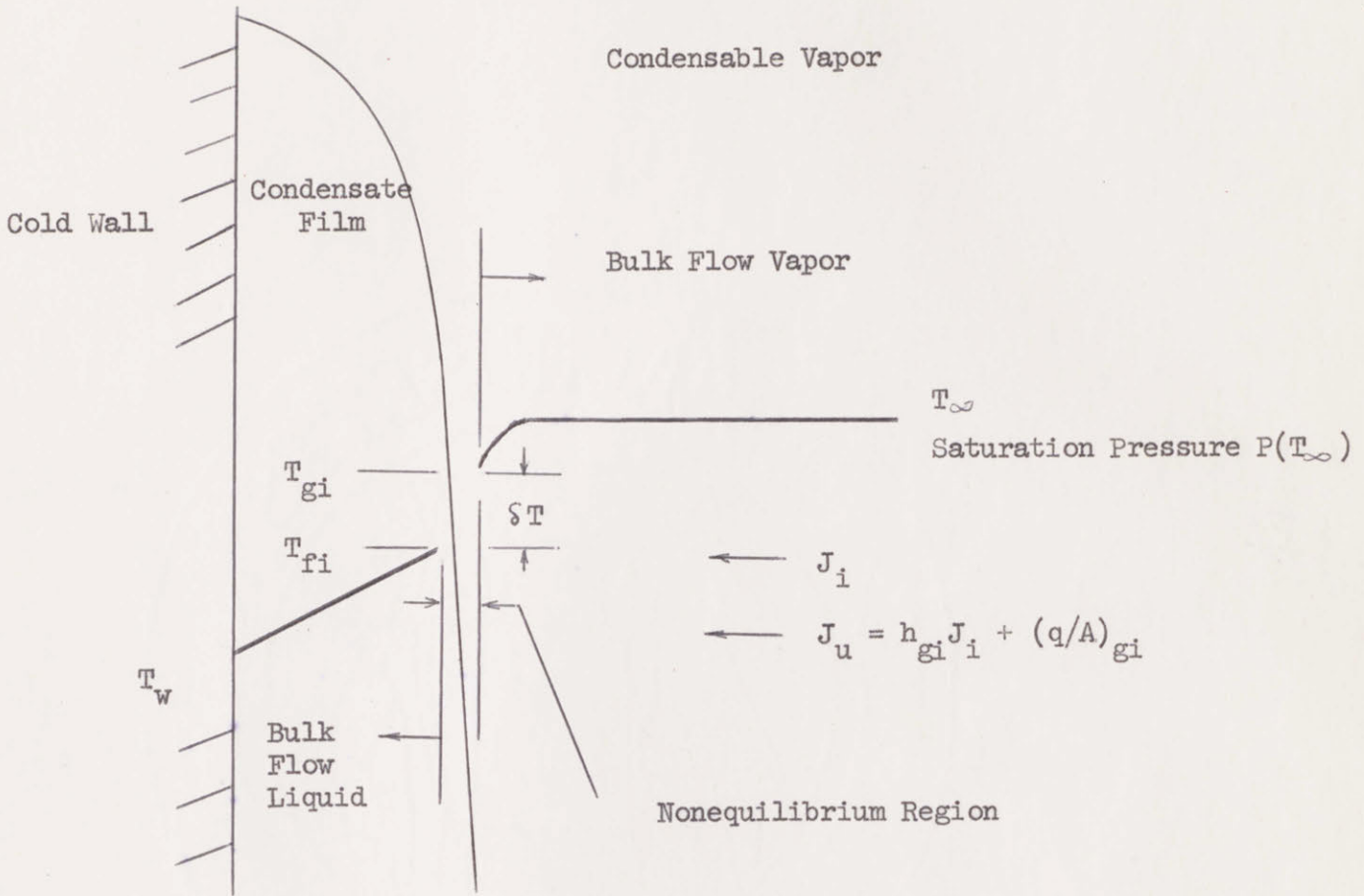


Figure 6 - Condensation Problem Including the Thermodynamic Analysis

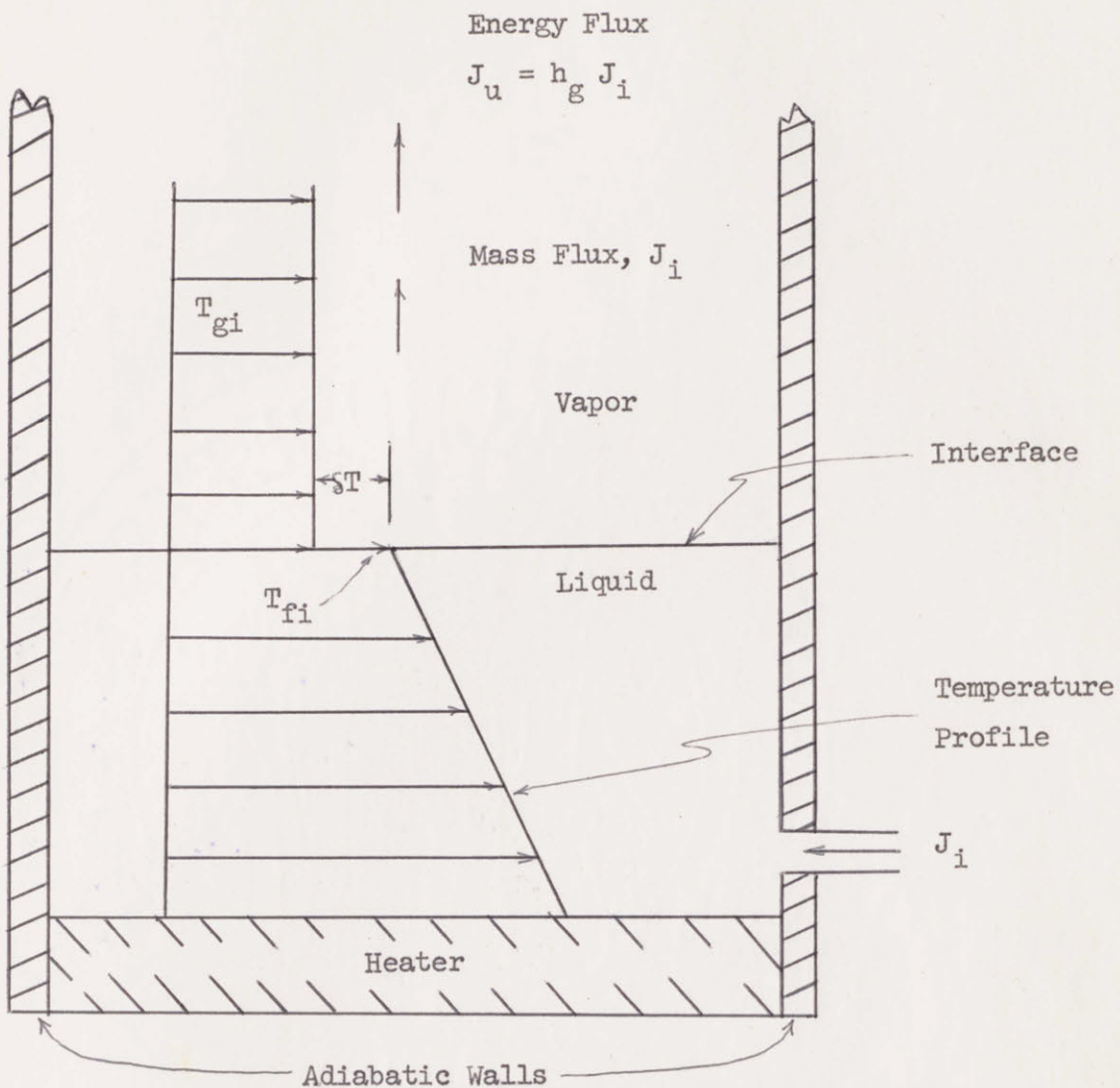


Figure 7 - Steady-State Evaporation Experiment

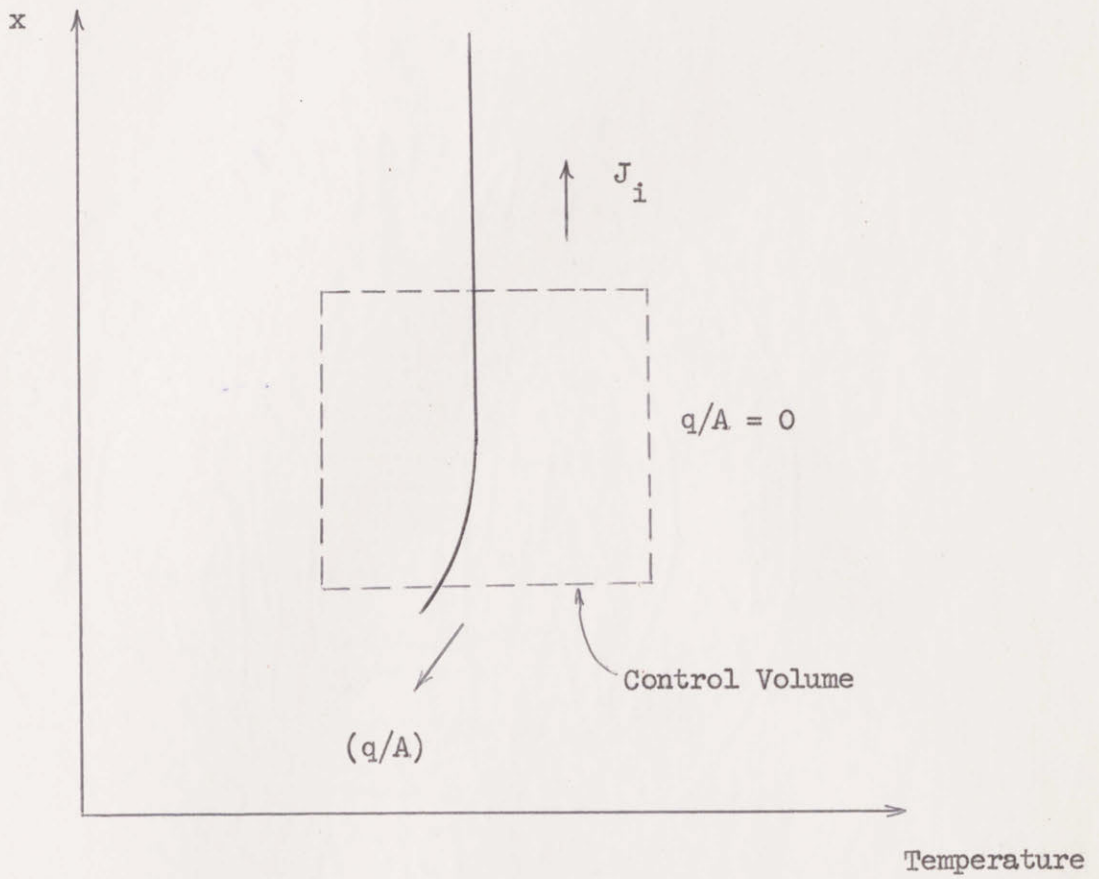


Figure 8 - First Law Consideration of Steady-State Evaporation Experiment

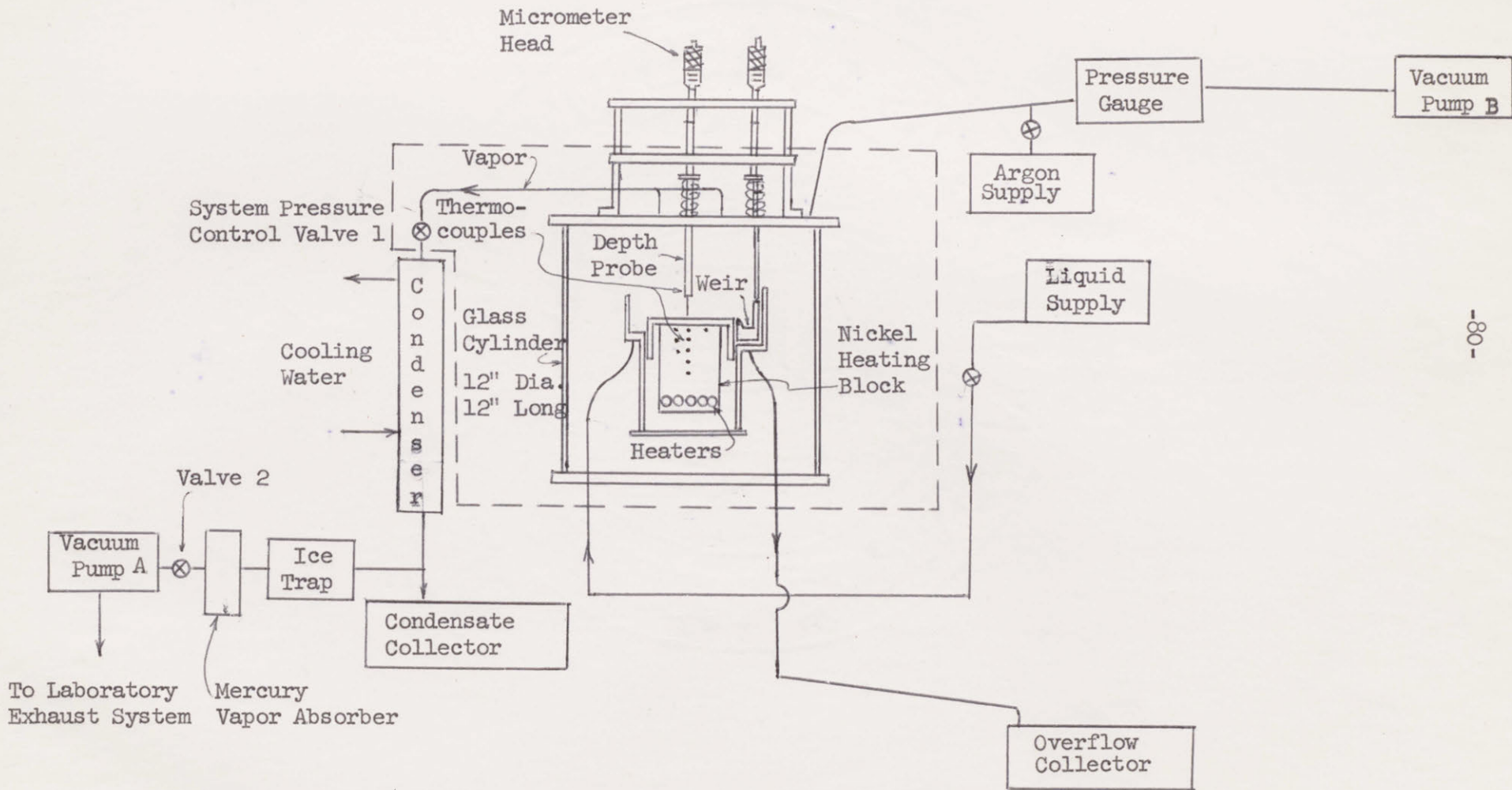


Figure 9 - Flow Diagram of Experiment

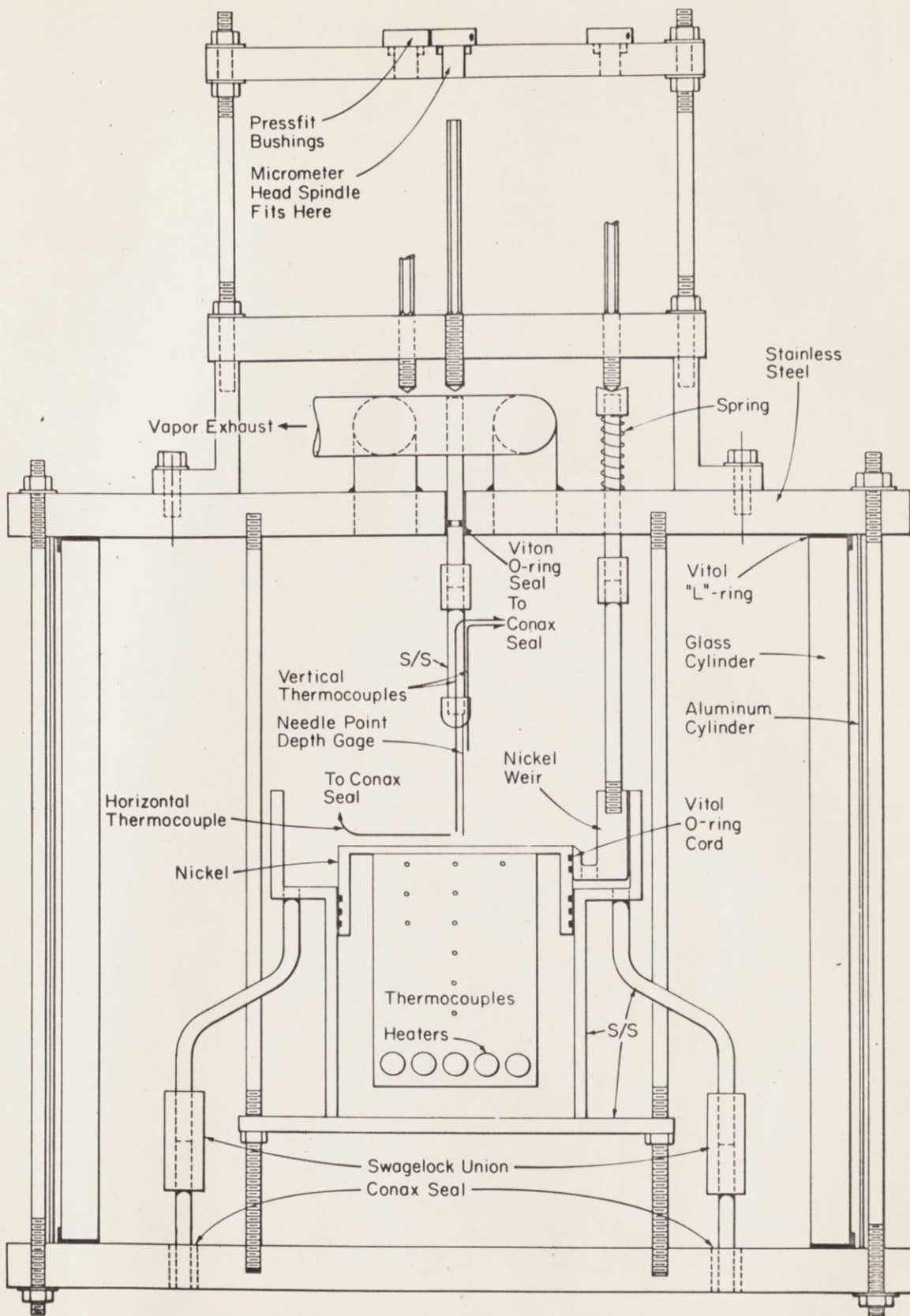


FIGURE 10 DRAWING OF TEST SECTION

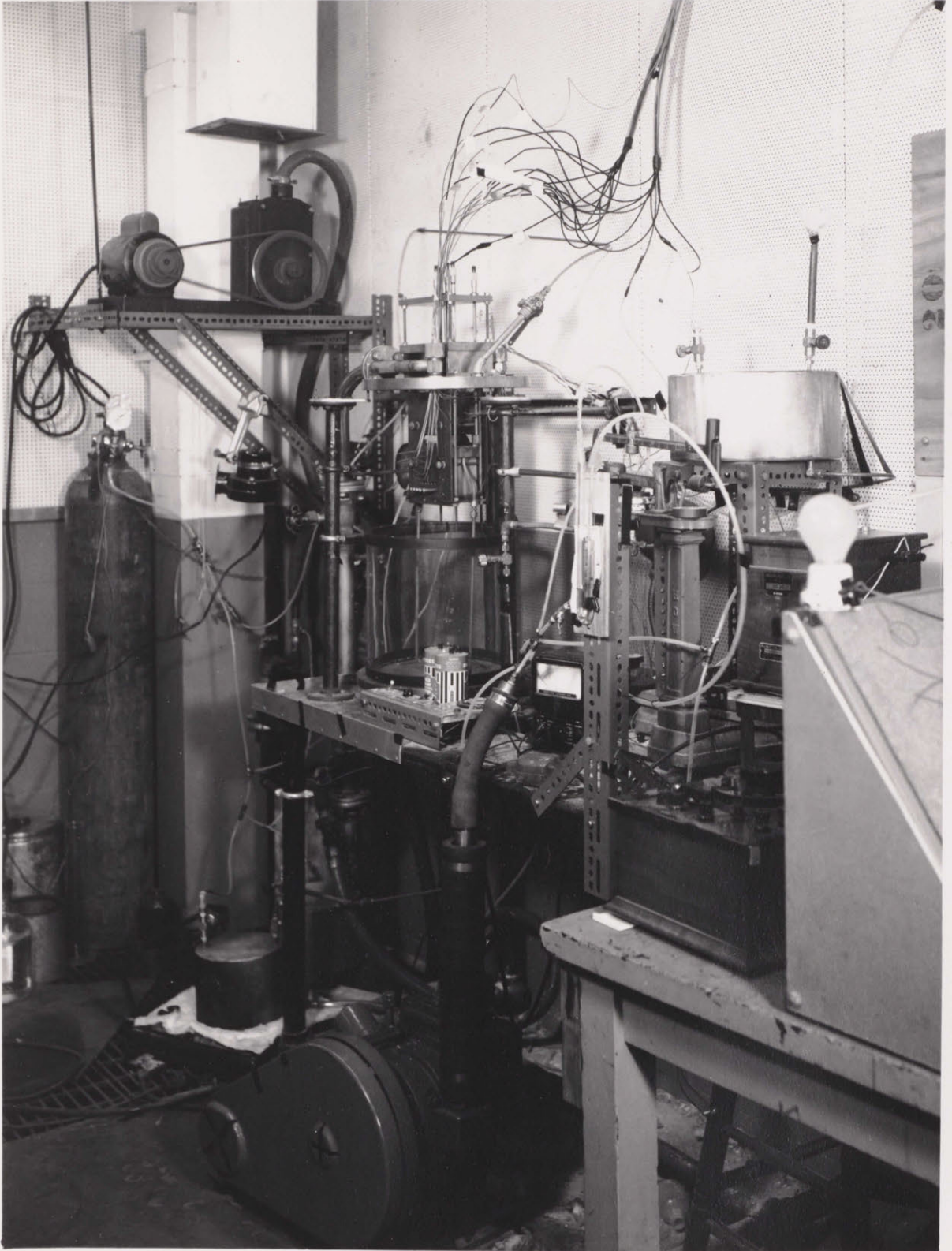


FIG. 11 PHOTOGRAPH OF EXPERIMENTAL APPARATUS

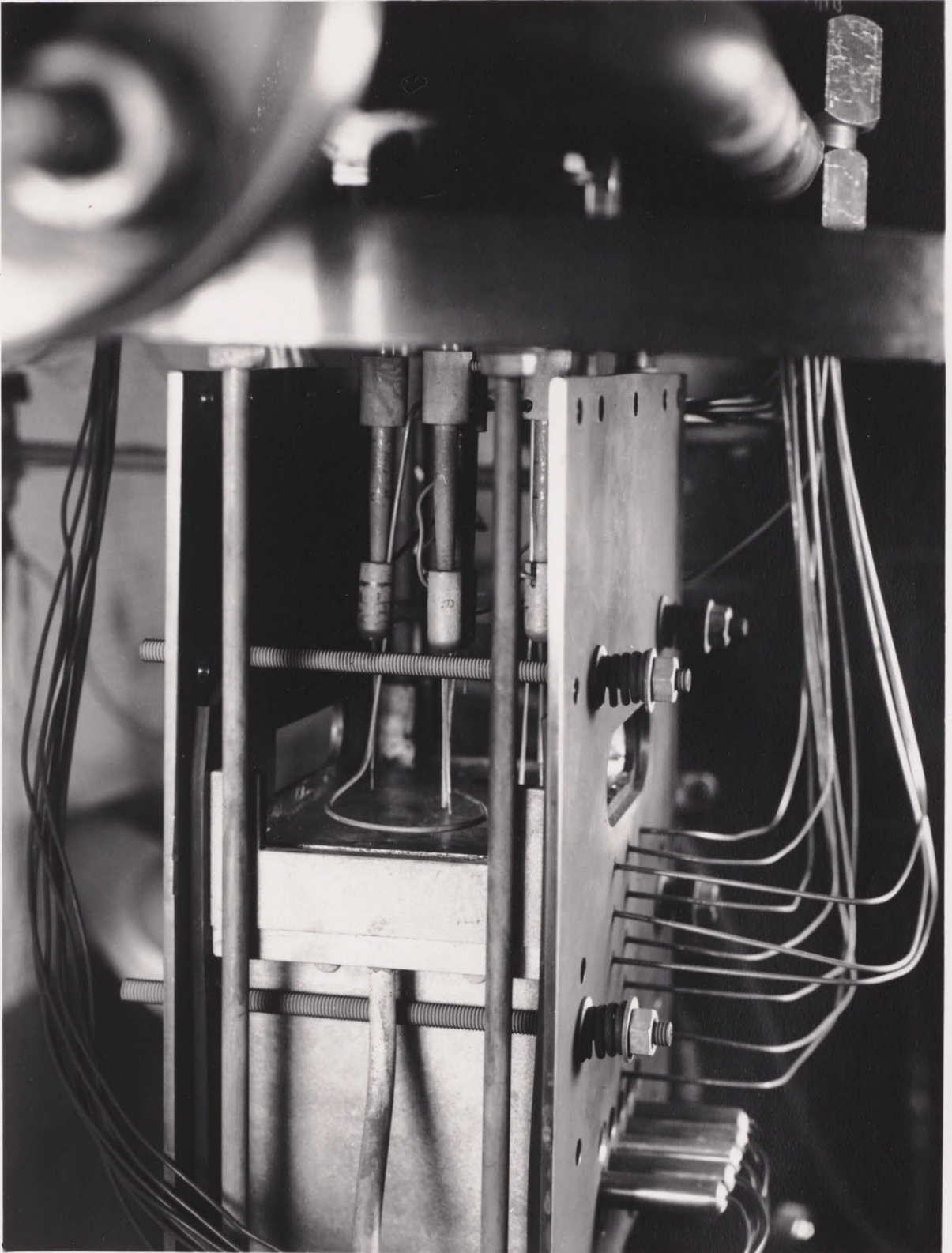


FIG. 12 PHOTOGRAPH OF TEST SECTION

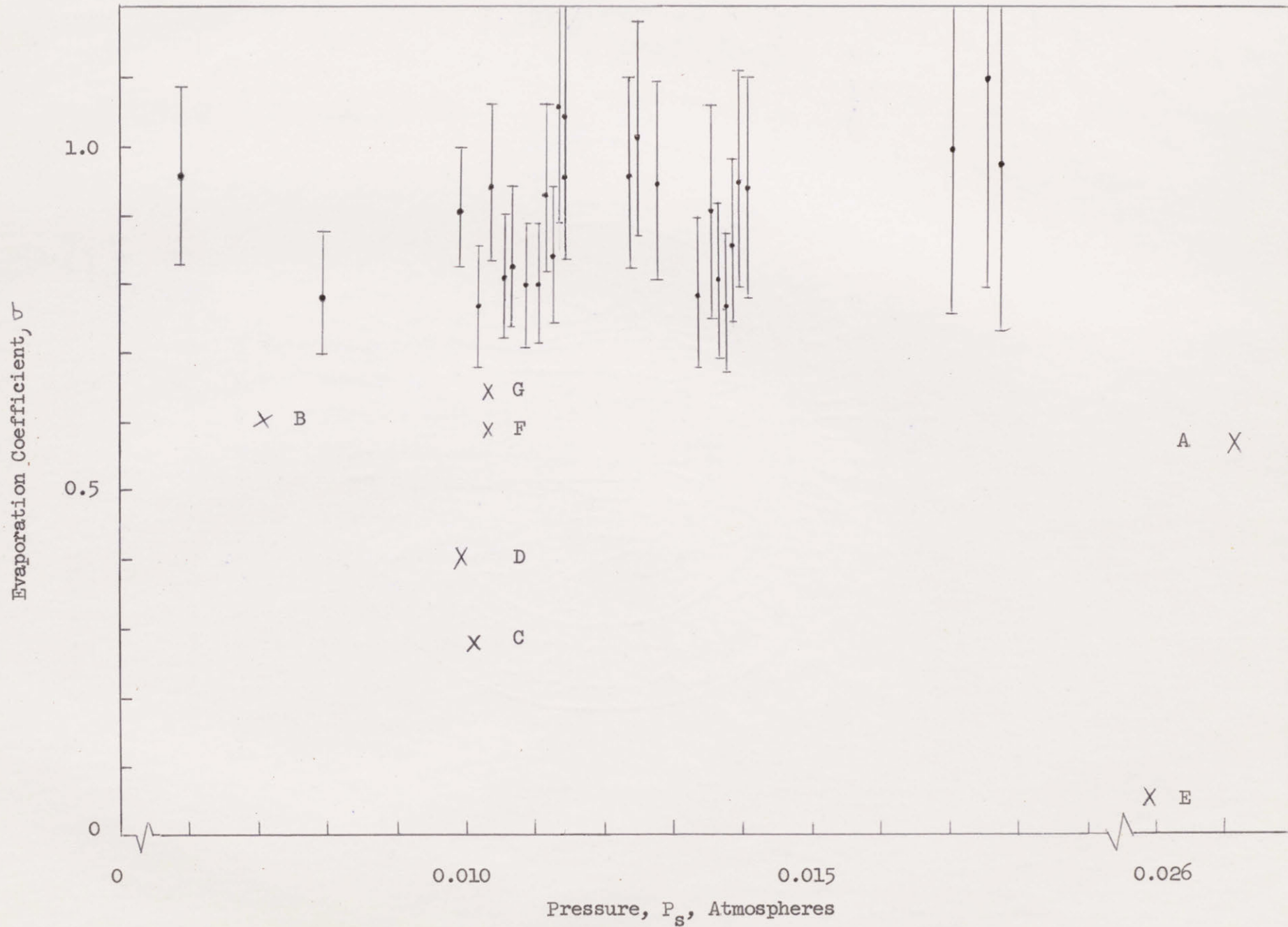


Figure 13 - Condensation Coefficient σ Versus Pressure P_s for Steady-State Evaporation Experiment

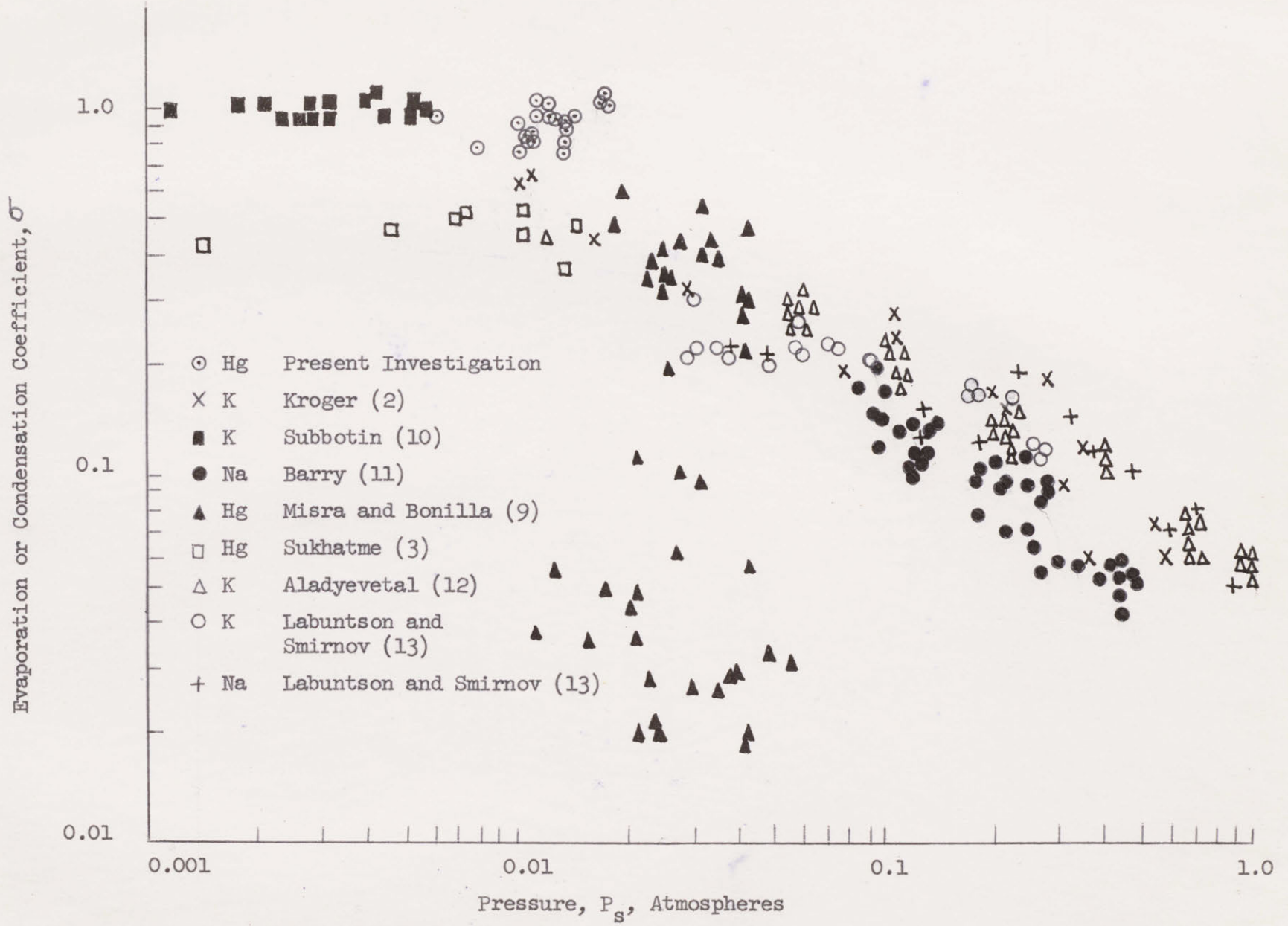


Figure 14 - Condensation Coefficient σ Versus Pressure P_s for Various Liquid Metals

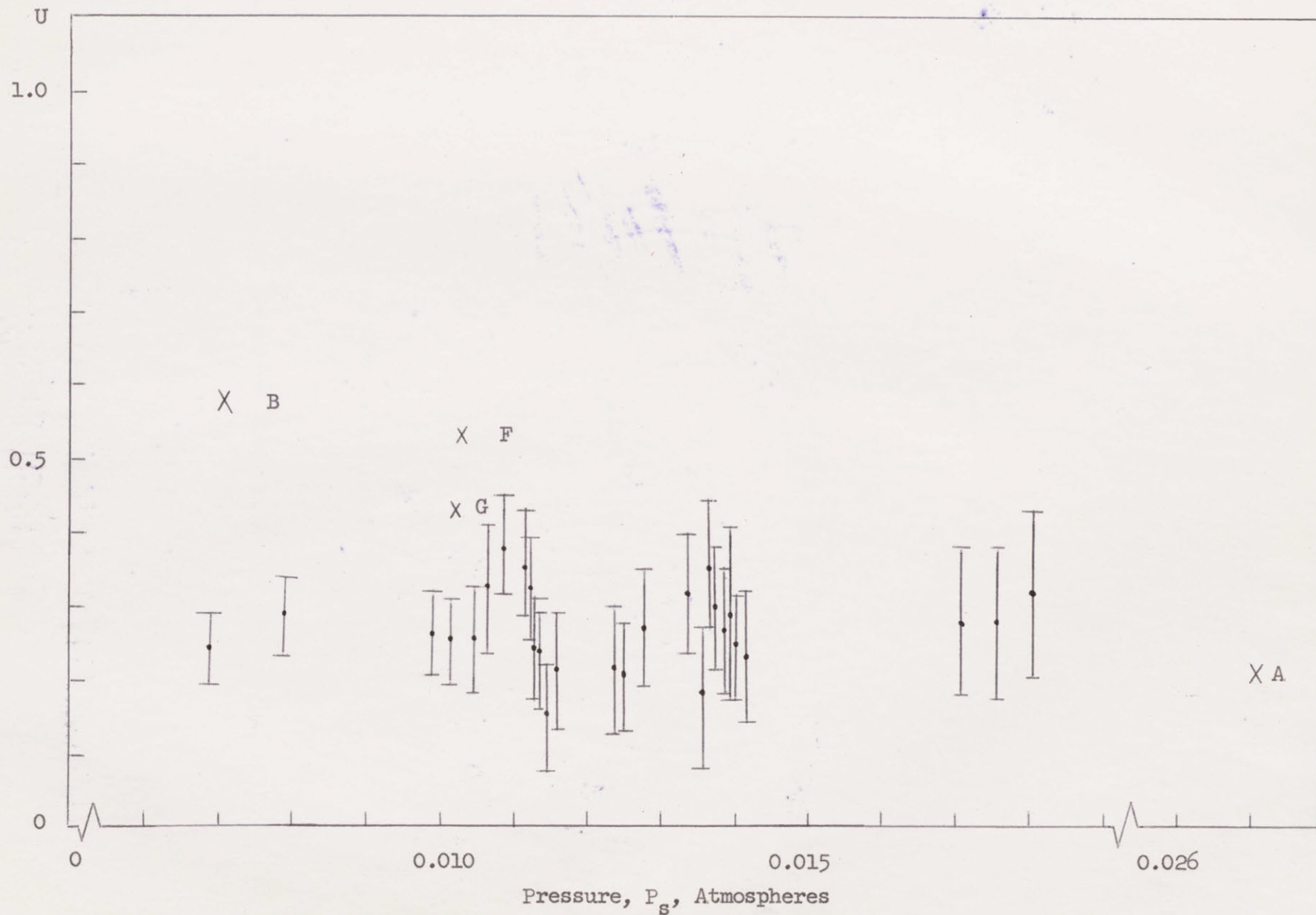


Figure 15 - U Versus Pressure P_s

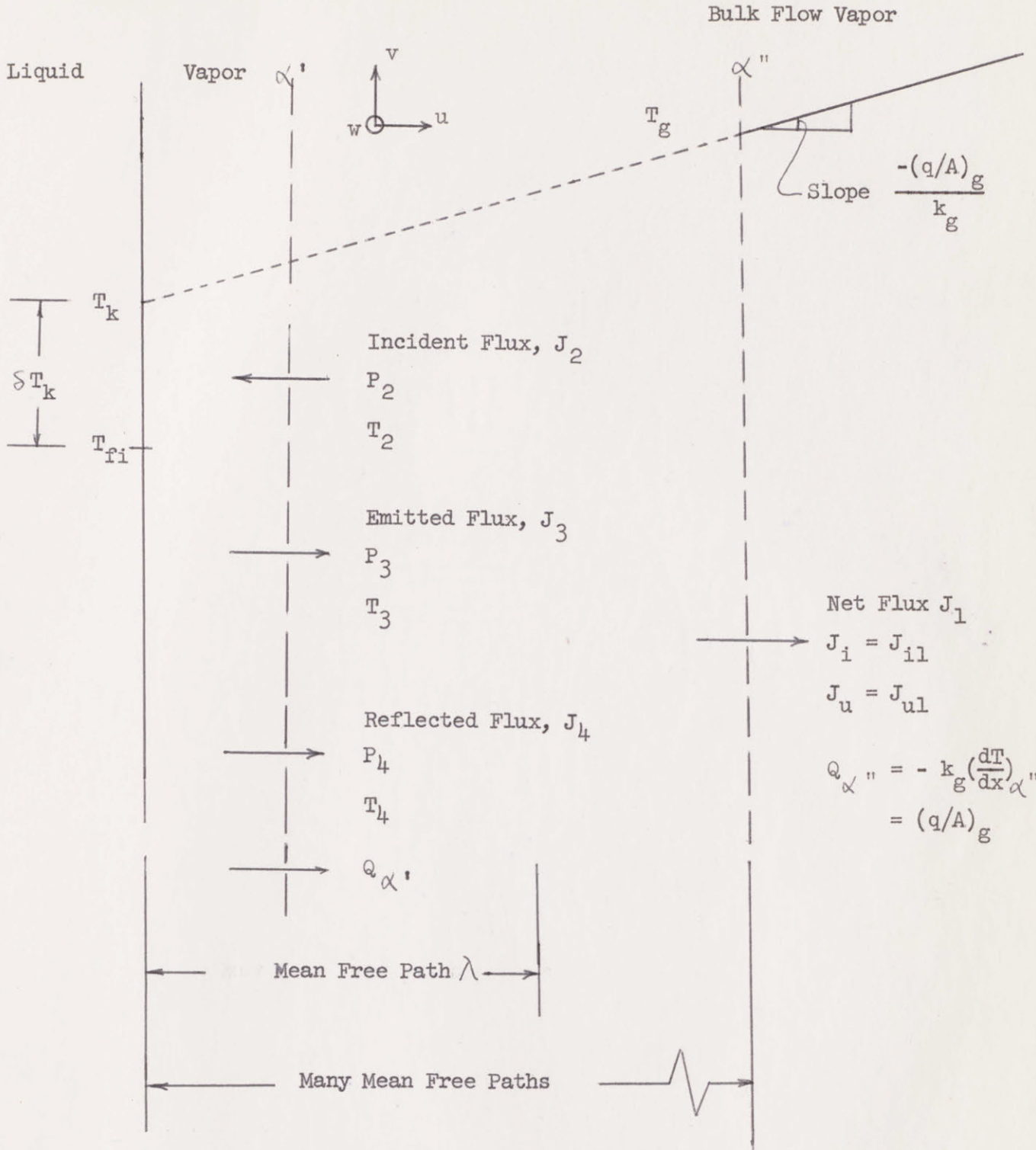


Figure 16 - General Kinetic Model of the Interface

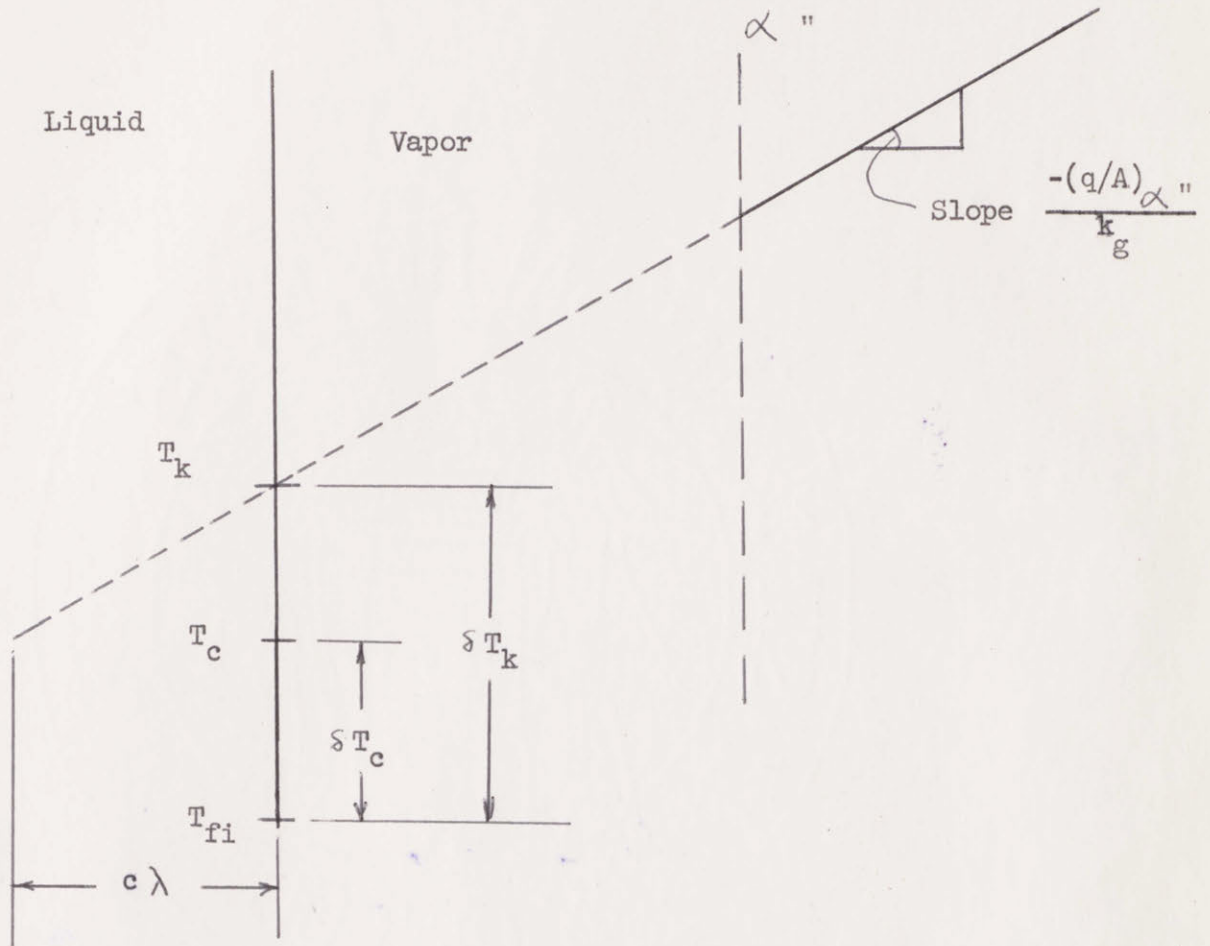


Figure 17 - Illustration of the Relationship Between δT_k and δT_c